nature neuroscience

ARTICLES

https://doi.org/10.1038/s41593-020-0600-3

Implicit adaptation compensates for erratic explicit strategy in human motor learning

Yohsuke R. Miyamoto[1], Shengxin Wang[2] and Maurice A. Smith[1,3] ✉

Sports are replete with strategies, yet coaching lore often emphasizes 'quieting the mind', 'trusting the body' and 'avoiding overthinking' in referring to the importance of relying less on high-level explicit strategies in favor of low-level implicit motor learning. We investigated the interactions between explicit strategy and implicit motor adaptation by designing a sensorimotor learning paradigm that drives adaptive changes in some dimensions but not others. We find that strategy and implicit adaptation synergize in driven dimensions, but effectively cancel each other in undriven dimensions. Independent analyses—based on time lags, the correlational structure in the data and computational modeling—demonstrate that this cancellation occurs because implicit adaptation effectively compensates for noise in explicit strategy rather than the converse, acting to clean up the motor noise resulting from low-fidelity explicit strategy during motor learning. These results provide new insight into why implicit learning increasingly takes over from explicit strategy as skill learning proceeds.

The human brain can engage both explicit and implicit mental processes, and these processes are used in combination when performing many different types of tasks, including foreign-language learning, driving, sequence learning and sensorimotor control[1–4]. These processes act in parallel and can work together to achieve successful performance, as explored in the popular book *Thinking Fast and Slow*[5], which summarizes a line of research led by Kahneman and Tversky on the contrast between two mental systems: (1) implicit thinking, which is intuitive and largely automatic and is referred to as System 1, and (2) explicit thinking, which is effortful and attention-demanding and is referred to as System 2. When playing chess, for example, you can make an intuitive move that just feels right or a more calculated move after meticulously analyzing the consequences of each possible action.

In the motor system, both implicit and explicit adaptations can be used to learn from errors in our actions. For example, after throwing a dart that misses to the left of the bullseye, one might strategically aim farther to the right for the next throw. However, an implicit adaptation would also occur such that even if one continued to aim at the bullseye, the dart would land progressively farther to the right.

The study of explicit aiming during reaching and pointing adaptation tasks has seen a recent surge in interest. In these tasks, aiming can be effective in compensating for visuomotor perturbations, whereby the relationship between hand motion and visual feedback of it is systematically altered. For visuomotor rotation learning in particular, in which participants receive directionally skewed visual feedback during reaching or pointing movements, explicit adjustment of one's aim point can result in near-complete compensation of the imposed rotation in just a few trials[4,6]. Studies have examined the effects of explicit strategies both by prescribing aim points[6–8] and by having participants compose and report their own strategies[4,9].

By contrast, implicit adaptation is a systematic change in motor output that occurs without conscious awareness. It has been extensively studied in visuomotor learning[6,10–13], prism adaptation[14,15] and force-field adaptation[16–21] paradigms, where it can result in large and prolonged aftereffects; that is, systematic changes in motor output that persist even after participants are made aware that the experimental manipulation has been removed. When perturbations are gradually introduced, participants will adapt while unaware of the perturbation[22–24], which indicates that adaptation can proceed entirely implicitly.

The coexistence of explicit and implicit learning raises the question of how these processes interact and potentially interfere with each other. Explicit strategy, which is thought to be driven by errors in performance[4,7,25], must depend on the level of implicit learning, as the amount of implicit learning will affect errors in performance. Meanwhile, current studies provide conflicting findings on the extent to which implicit learning depends on the use of explicit strategies. Some work has claimed that participants provided with an explicit strategy exhibit the same amount of implicit adaptation as those who are not[6], which suggests that implicit learning proceeds independently of strategy[11]. However, other studies have found that participants who are provided with an explicit strategy in fact display significantly attenuated implicit learning[8,26], which suggests instead that explicit strategies interfere with implicit learning.

When individuals create their own explicit strategies and continually adjust them, it is clear that strategic and implicit adaptation proceed in a highly complementary fashion, with strategy levels rapidly increasing at first, but then slowly receding in step with the slow increases in implicit adaptation such that the combined adaptation is maintained[4,9]. This complementarity suggests that there are antagonistic interactions between implicit and strategic learning, such that when one is high, the other becomes low. But it is not clear whether this interaction arises because strategy responds to changes in implicit learning or because implicit learning responds to changes in strategy or a combination of these two effects.

To understand how strategy and implicit learning interact during motor adaptation, we created a task in which we could measure how implicit and strategic learning change from one trial to the next while continually driving motor adaptation via visuomotor perturbations that constantly evolve throughout training. However, while perturbations are crucial for driving motor adaptation, their presence makes it difficult to disentangle internal interactions from

[1]John A. Paulson School of Engineering and Applied Sciences, Harvard University, Cambridge, MA, USA. [2]Department of Mechatronics Engineering, Harbin Institute of Technology, Harbin, China. [3]Center for Brain Science, Harvard University, Cambridge, MA, USA. ✉e-mail: mas@seas.harvard.edu

responses driven by external perturbations because individual adaptive processes will respond not only to each other but also to the perturbation itself. On the other hand, eliminating perturbations would remove the drive for learning, extinguishing adaptive responses and thereby make their interactions difficult to systematically investigate. We therefore designed a paradigm that allowed us to observe implicit learning and strategy simultaneously in perturbation-driven and perturbation-free dimensions. This paradigm allowed us to decompose adaptive responses into separate channels and to apply perturbations to some channels but not others to drive adaptation in the perturbed channels and, simultaneously, isolate the interactions between processes in the unperturbed channels.

Using this approach, we discover that implicit learning and strategy interact in a synergistic, positively correlated manner in perturbation-driven channels, but in an antagonistic, negatively correlated manner in perturbation-free channels. The antagonistic responses in perturbation-free channels suggest that one process can correct for the other to reduce the performance errors in the net behavior. Through multiple convergent analyses and simulations, we demonstrate that implicit learning compensates for the performance errors induced by strategy rather than the converse.

Results

To understand how implicit and strategic learning interact during motor adaptation, we trained participants ($n=41$) on a task that allowed us to measure how implicit learning and strategy evolve throughout the course of training. Like the classical visuomotor rotation task[6,10,11,13,21], participants were instructed to move a cursor that responded to hand motion toward a target when the cursor motion was rotated relative to hand motion (Fig. 1a). This required participants to adapt the direction of hand motion to counteract the rotation. Critically, participants in our task were free to use an explicit aiming strategy to improve performance. Before each movement, participants positioned a marker at the aim point that they thought would facilitate accurate cursor movement toward the target. This aiming marker provided visual guidance for the participant and provided us with a measurement of the aiming strategy for each trial, which then allowed us to decompose the combined adaptation into strategic versus implicit components for each movement to monitor how strategy, implicit learning and combined learning evolved from one movement to the next throughout training (Fig. 1a). We operationally defined strategic learning as the angular displacement between the aiming direction and the target, while implicit learning was defined as the displacement between the direction of hand motion and the aiming direction.

A key feature of our task was the design of a visuomotor rotation sequence that continually evolved to drive motor adaptation and stimulate interactions between learning processes throughout the course of training. However, even with the continual stimulation enabled by such a perturbation, understanding the interactions between implicit and strategic learning is challenging. This is because individual adaptive processes can respond to both the perturbation and to each other, making it difficult to isolate interactions. Removing the perturbation would expose the interactions; however, this would also remove the drive for overall adaptation, decimating the adaptive responses for both implicit learning and strategy and making interactions between them difficult to resolve.

To address these issues, we designed a visuomotor rotation sequence that not only evolved throughout training but also allowed us to observe both perturbation-driven and perturbation-free responses simultaneously. For perturbation-driven responses, a perturbation is present to drive strategic learning, implicit learning and their interactions, whereas for perturbation-free responses, no perturbation is present to drive strategic or implicit learning so that interactions were more readily isolated. To accomplish this, we constructed a perturbation sequence out of sinusoidal components at different frequencies, but used only a subset of the available frequencies[27,28] (the 'sum-of-sines' sequence; Fig. 1b,c). Summing sinusoidal perturbation sequences resulted in a composite sequence that evolves over time in a smooth but complex manner. We can efficiently represent this perturbation sequence using the amplitudes and phases of sinusoids at different frequencies because perturbations appear only at a few select frequencies (Fig. 1d). Notably, this frequency-based representation separates out the adaptive responses at perturbed frequencies (perturbation-driven responses) from those at unperturbed frequencies (perturbation-free responses), and each parameter in it was independent of the others because of the orthogonality of sine waves at different frequencies.

A sum-of-sines perturbation sequence elicits similar levels of implicit and explicit adaptation and enables the dissection of adaptive responses into perturbation-driven and perturbation-free responses. Participants experienced a visuomotor rotation sequence composed of 5 sinusoidal components, with periods of 48, 96, 192, 384 and 768 trials (corresponding to frequencies of 16, 8, 4 and 2 cycles and 1 cycle, respectively, in the 768-trial training period), each with 10° of amplitude (Fig. 2a, black dashed line). The sequence continually evolves over the course of training, from rotations as low as −30° to as high as +30° but gradually, with trial-to-trial changes no larger than 2.53° in magnitude and an average of 1.07° root mean squared (r.m.s.).

Participants readily adapted to the sum-of-sines visuomotor perturbation, with individual performance values that resulted in r.m.s. errors of 5.76 ± 0.19° (mean ± s.e.m. across participants) compared with the 15.8° r.m.s. error that was expected if no adaptation had occurred. The mean combined learning closely followed the shape of an ideal learning pattern, with an error of 2.77° r.m.s. (Fig. 2a, purple solid line versus black dashed line). Decomposing the combined learning curve into implicit learning and strategy components (Fig. 2c) revealed that both of these components closely approximated the shape of the ideal learning curve ($r=0.94$ and $r=0.95$ for participant-averaged implicit learning and strategic learning, respectively) and displayed similar r.m.s. amplitudes (11.12 ± 0.32° versus 9.05 ± 0.74°, respectively). This indicates that the sum-of-sines perturbation paradigm strongly stimulated both implicit and strategic learning throughout the course of training.

We examined how learning varied across different frequencies to separate out adaptive responses into perturbation-driven and perturbation-free parts. For combined learning (implicit + strategy), perturbation-driven frequencies (Fig. 2b, purple stars) exhibited mean response amplitudes more than 20-fold greater than perturbation-free frequencies or, more specifically, perturbation-free frequencies in the same frequency range, 1–16 cycles in the experiment (8.99 ± 0.08° versus 0.33 ± 0.02°, $t(40)=100.3$, $P<1\times10^{-48}$ or versus 0.37 ± 0.02°, $t(40)=93.4$, $P<1\times10^{-47}$). Note that these responses are similar to those expected from ideal learning: 10° at perturbation-driven frequencies and 0° at perturbation-free frequencies.

Similarly, we found that individual responses in implicit learning and explicit strategy both displayed adaptive responses that were greater at perturbation-driven frequencies (5.31 ± 0.25° and 4.47 ± 0.38°, respectively) than at perturbation-free frequencies. We found similar results when comparing against perturbation-free frequencies in the same frequency range (1.04 ± 0.11°, $t(40)=13.0$, $P<1\times10^{-15}$ and 1.04 ± 0.10°, $t(40)=11.4$, $P<1\times10^{-13}$, for implicit learning and strategy, respectively) and against all perturbation-free frequencies (0.33 ± 0.03°, $t(40)=19.2$, $P<1\times10^{-21}$ and 0.24 ± 0.02°, $t(40)=11.6$, $P<1\times10^{-13}$, respectively).

Implicit learning and strategy are synergistically aligned and display complementary amplitudes at perturbation-driven frequencies. We next investigated the interactions between implicit learning and strategy for perturbation-driven responses. We found

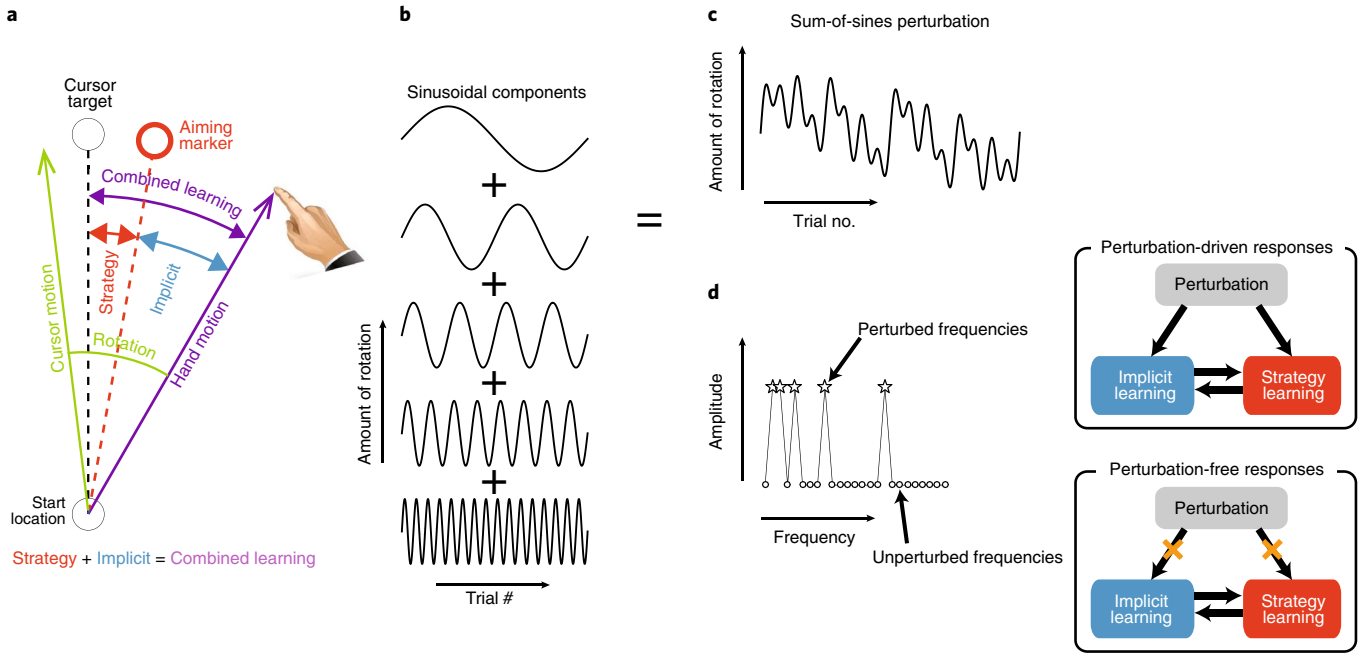

Fig. 1 | Experimental setup. a, Set up of the aiming-based visuomotor rotation task to measure strategy and implicit learning. Before each reaching movement, participants indicated their aiming strategy by positioning an aiming marker (large red ring) to guide the reach. Explicit strategy (red double-headed arrow) was operationally defined as the difference between the aiming direction (red dashed line) and cursor target direction (black dashed line). Implicit learning (blue double-headed arrow) was operationally defined as the difference between the hand direction (purple arrow) and aiming direction (red dashed line). Strategy and implicit learning together sum to the combined learning (purple double-headed arrow), which amounts to the difference between the hand direction (purple arrow) and the cursor target direction (black dashed line). During the visuomotor rotation task, the size of the perturbation determines the amount of rotation between the displayed cursor motion (green arrow) and the hand direction (purple arrow). **b**,**c**, Sum-of-sines composition of the visuomotor rotation sequence. Participants experienced a visuomotor rotation perturbation sequence composed of sine-shaped components at select frequencies (**b**), resulting in a continually changing perturbation (**c**). **d**, Illustration of a frequency space representation of perturbation. Here, the visuomotor rotation sequence is represented as rotation amplitude as a function of frequency rather than rotation as a function of time. At perturbed frequencies (stars), we observe perturbation-driven responses that reflect not only the interactions between implicit and strategic learning but also their responses to the perturbation. At unperturbed frequencies (circles), we observe perturbation-free responses that reflect only interactions between processes.

that the combined adaptation was substantially higher than both the implicit and strategic adaptation at perturbation-driven frequencies (Fig. 3a; $t(40)=14.9$, $P<1\times10^{-17}$ and $t(40)=11.6$, $P<1\times10^{-13}$), which suggests that the implicit and strategic responses are aligned so that they combine synergistically at perturbation-driven frequencies. This alignment, as evidenced by a positive correlation between the learning curves for implicit and strategic adaptation, is apparent in the example data for a participant shown in Fig. 3c, as these two curves largely increase and decrease together ($r=+0.66$), and in the group data (Fig. 3d; $r=+0.57\pm0.07$ (mean ± s.e.m.), $t(40)=8.68$, $P<1\times10^{-10}$).

The observed alignment between the implicit and strategic adaptive responses at perturbation-driven frequencies is in line with the idea that implicit and strategic adaptation cooperate to effectively counteract the perturbation. Such cooperation would further predict that the amount of implicit and strategic adaptation complement one another to achieve a level of combined adaptation that is close to ideal. This can be seen in two different ways in our data. First, in the highly complementary relationship between the levels of implicit and strategic learning when compared across individual participants after being combined across perturbation-driven frequencies (Fig. 3e; $r=-0.88$, $F(1, 39)=139.5$, $P<1\times10^{-13}$). Specifically, individuals were highly consistent in the amount of combined learning (implicit + strategy) they achieved, which is represented by the direction orthogonal to the diagonal ideal-learning manifold. But they varied widely in how this combined learning is achieved along the ideal-learning manifold using implicit versus strategic learning. That is, some individuals displayed high implicit but low explicit learning while others displayed high explicit but low implicit learning. Second, in the complementary relationship between the levels of participant-averaged implicit and strategic learning across perturbation-driven frequencies (Fig. 3a). Here, the combined adaptation remained nearly constant across frequencies, despite large changes in the amount of implicit and strategic learning. In particular, strategic learning dominated at higher frequencies that required rapid changes in adaptation, which is in line with high learning rates for strategy, whereas implicit learning was systematically stronger at lower frequencies, perhaps due to higher retention for implicit adaptation. This results in the apparent X-shaped pattern shown in Fig. 3a, where implicit learning increases with frequency (slope $=+4.62\pm0.58$, $t(40)=7.94$, $P<1\times10^{-9}$), strategic learning decreases with frequency (slope $=-3.76\pm0.63$, $t(40)=6.02$, $P<1\times10^{-6}$) and the two are negatively correlated ($r=-0.77\pm0.07$). Thus, as implicit learning rises, strategic learning falls in a complementary fashion to achieve nearly constant combined learning.

Implicit learning and strategy are antagonistically aligned and closely matched in amplitude to effectively cancel each other out at perturbation-free frequencies. The synergistic relationship between implicit and strategic learning observed at perturbation-driven frequencies was in sharp contrast to their relationship at perturbation-free frequencies. For the perturbation-free responses in the same frequency range as the perturbation-driven responses (1–16 cycles in the training period), combined learning was not

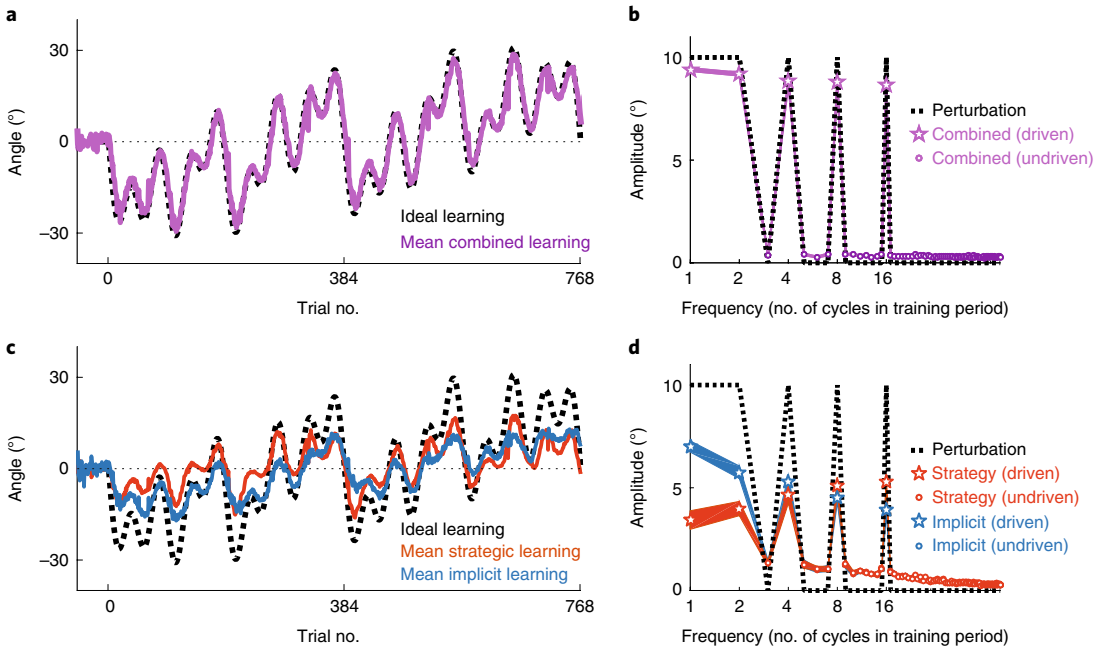

Fig. 2 | Learning curves and frequency space representations of implicit, strategic and combined learning. a,**c**, Population-averaged learning curves. Over the course of the 768-trial training period, mean combined learning (**a**) and implicit and strategic learning (**c**) closely track the pattern of ideal learning (black dashed line) that would be required for participants to fully counteract the visuomotor rotation sequence. Trial 0 indicates the onset of the visuomotor rotation. **b**,**d**, Population-averaged amplitudes across different frequencies. Amplitudes are shown for the rotation sequence (black dashed line), combined learning (**b**), and implicit learning and strategic learning (**d**). Note that these panels display the mean of individual participants' amplitudes for each frequency rather than the amplitude of the mean response across individual participants. Frequency is displayed as the number of cycles per 768 trials (the length of the training period). Stars indicate responses at perturbation-driven frequencies and circles indicate responses at perturbation-free frequencies. The vertical thickness of the shaded regions indicates the s.e.m.

larger but smaller than either implicit or strategic learning in isolation (Fig. 3b; $0.48 \pm 0.03°$ versus $1.32 \pm 0.15°$, $t(40) = 5.49$, $P < 1 \times 10^{-5}$ or $1.27 \pm 0.15°$, $t(40) = 5.10$, $P < 1 \times 10^{-5}$). This results from the fact that implicit and strategic responses are strongly negatively correlated ($r = -0.87 \pm 0.02$, $t(40) = 40.7$, $P < 1 \times 10^{-33}$) so that they largely oppose one another and interact antagonistically rather than synergistically. This antagonistic interaction is readily apparent in the example learning curves of a participant, in which implicit and strategic adaptations effectively canceled one another because they displayed negatively correlated time courses, oscillating in opposition (Fig. 3f; $r = -0.92$).

Cancellation between implicit and strategic learning would be especially effective if these responses were not only negatively correlated and therefore oppositely directed but also closely matched in amplitude. We found two pieces of evidence to indicate that this is indeed the case at low perturbation-free frequencies (1–16 cycles in the training period). First, when the implicit and strategic adaptations were combined across these frequencies, they were closely matched in amplitude across individuals (Fig. 3h; slope $= 1.04 \pm 0.09$, $r = +0.99$, $F(1, 39) = 1431.4$, $P < 1 \times 10^{-31}$). This was also the case in the four-frequency and seven-frequency datasets ($r = +0.97$, $F(1, 12) = 182.7$, $P < 1 \times 10^{-7}$ and $r = +0.90$, $F(1, 12) = 52.7$, $P < 1 \times 10^{-4}$, respectively). Conversely, when combined across participants, the implicit and strategic adaptations were closely matched in amplitude across frequencies (Fig. 3b; similar values between red and blue circles at each perturbation-free frequency: $r = 0.68 \pm 0.06$, $t(40) = 12.2$, $P < 1 \times 10^{-14}$ where the correlation across frequencies is calculated for each participant).

To test the robustness of the dichotomy between synergistic and antagonistic interactions, we ran additional experiments in which we trained participants on sum-of-sines perturbations that contained different numbers of frequencies and different frequency ranges. In these experiments, we trained 14 participants on a 384-trial perturbation sequence that was constructed from 4 sinusoidal components with 1, 2, 4 and 8 cycles (corresponding to periods of 384, 192, 96 and 48 trials, respectively) each with 10° of amplitude, and another 14 participants on a 768-trial perturbation sequence that was constructed from 7 sinusoid components with 2, 4, 8, 16, 32, 64 and 128 cycles (corresponding to periods of 384, 192, 96, 48, 24, 12 and 6 trials, respectively) also each with 10° of amplitude. Similar to the main five-frequency experiment, we found systematically positive correlations between implicit and strategic learning curves at the perturbation-driven frequencies ($r = +0.72 \pm 0.04$ and $r = +0.41 \pm 0.15$ for the four-frequency and seven-frequency experiments, respectively, with $t(13) = 19.1$, $P < 1 \times 10^{-10}$ and $t(13) = 2.80$, $P = 0.015$, respectively), which indicates that there is synergistic alignment between them. Correspondingly, we found systematically negative correlations between implicit and strategic learning curves at the perturbation-free frequencies in these experiments ($r = -0.21 \pm 0.09$, $t(13) = 2.43$, $P = 0.03$ for four-frequency and $r = -0.38 \pm 0.10$, $t(13) = 3.86$, $P < 0.01$ for seven-frequency). These results reinforce the findings that implicit and strategic learning act synergistically at perturbation-driven frequencies, but antagonistically at perturbation-free frequencies,

But why would the learning curves for implicit and strategic learning be in opposition to one another? Antagonistic interactions, whereby implicit and strategic learning largely cancel out one another, improve performance at the perturbation-free frequencies because the ideal adaptation at these frequencies is zero, and any net adaptation would increase motor error. This suggests that implicit or strategic adaptation may actively compensate for the other from one trial to the next as adaptation proceeds. If so, active compensation would be most effective at low frequencies (where the slow changes in activity would be easy to track), less effective at

intermediate frequencies and largely ineffective at higher frequencies (where fast changes in activity would be challenging to track). In line with this expectation, the antagonistic alignment between implicit and strategic learning was strongest at the lowest frequencies (Fig. 3f,g; $r=-0.87\pm0.02$), weaker at medium frequencies (Fig. 3i,j; $r=-0.70\pm0.04$, $t(40)=17.8$, $P<1\times10^{-19}$ when comparing low to medium frequencies) and essentially absent at high frequencies (Fig. 3k,l; $r=0.02\pm0.05$, $t(40)=0.32$, $P=0.75$). Note that the large changes in correlation across frequency bands is at odds with the possibility that the antagonistic alignment we observed arises from measurement noise, which would lead to negative correlations, but at low, medium and high frequencies.

If implicit or strategic adaptation actively compensates for the other at perturbation-free frequencies, the process that is compensated would display a pattern across trials that was consistent across individuals or idiosyncratic. The former would suggest that something about the task or perturbation sequence is the main driver, and the latter would indicate a sporadic source, such as sensorimotor noise. We found that at perturbation-free frequencies, the amplitudes of the participant-averaged adaptation were far smaller than the mean amplitude of the individual participant adaptation (small dots versus circles in Fig. 3b; 0.08° versus 0.34°, 0.07° versus 0.25°, 0.08° versus 0.34° for implicit, strategic and combined learning, respectively, and with differences of 345%, 242% and 307%, respectively). An analysis of this effect indicated that the consistent part constituted only 4% of the variance in implicit adaptation for individual participants and about 8% for strategic adaptation. This was in contrast to data from perturbation-driven frequencies, for which participant-averaged responses and the mean amplitude of the individual participant responses were similar, thereby indicating that the vast majority of the responses of the individual participants were consistent (dashed line versus stars in Fig. 3a; 4.8° versus 5.3°, 4.3° versus 4.5°, 9.0° versus 9.0°, for implicit, strategic and combined amplitudes averaged across all perturbation-driven frequencies, respectively, and with differences of 11%, 4% and 0.1%, respectively). Thus, whereas adaptive responses at perturbation-driven frequencies are strikingly similar, which is in line with a common perturbation sequence eliciting them, adaptive responses at perturbation-free frequencies are highly idiosyncratic, which is in line with the idea that a common perturbation has little effect at perturbation-free frequencies. Consequently, idiosyncratic sensorimotor noise is the main driver of the inappropriate adaptation being compensated. But which process is compensating for which? Is strategy primarily canceling out inappropriate implicit learning or is implicit learning primarily canceling out inappropriate strategy?

Analysis of the amplitudes of implicit and strategic learning indicates that implicit learning compensates for strategy. Next, we investigated whether the cancellation we observed between implicit and strategic learning at the perturbation-free frequencies arose from implicit learning responding to strategy, the reverse or a combination of the two. To accomplish this, we began with an analysis based on structural equation modeling (SEM; also referred to as path analysis) on the amplitude data for the perturbation-driven and perturbation-free implicit and strategic learning across individuals. SEM estimates the connection strengths within a network of variables. Applications range from estimating genetic versus environmental influences on phenotypic traits in genetics[29] to functional connectivity between brain areas in functional magnetic resonance imaging data in neuroscience[30]. Based on the covariance structure of the data, this analysis compares different models of how information flows between variables of interest.

Here, we employed SEM to examine the flow of information between perturbation-driven and perturbation-free strategic and implicit learning. We compared four structural equation models: a baseline model without any interaction between implicit and strategic learning, and three models with different types of interactions, as illustrated in Fig. 4. We evaluated these models by pooling together the data across the five-, four- and seven-frequency perturbation experiments and calculating the log-likelihood associated with the

Fig. 3 | Strategy and implicit learning synergize at perturbation-driven frequencies, but cancel at perturbation-free frequencies. a, Amplitudes at perturbation-driven frequencies. The stars, connected by solid lines, indicate the mean individual participant amplitudes at perturbation-driven frequencies for strategic, implicit and combined learning. The dotted lines, in contrast, indicate the amplitude of the mean response across individual participants. Note that the purple dotted line largely overlaps with the purple solid line. The horizontal black dashed line at 10° indicates the amplitude that would be expected from ideal learning. **b**, Amplitudes at perturbation-free frequencies. The circles indicate the mean of individual participant amplitudes at perturbation-free frequencies for strategic, implicit and combined learning. The small dots, in contrast, indicate the amplitude of the mean response across individual participants. The gray vertical stripes indicate the perturbation-driven frequencies to depict the range of perturbation-driven frequencies. **c**, Time courses of perturbation-driven responses for an example participant. Learning curves of an example participant for perturbation-driven frequencies show that strategic and implicit learning curves are strongly aligned and synergistically combine to form the combined learning curve. The thick black dashed line indicates the time course for ideal learning. **d**, Distribution of correlations between perturbation-driven implicit and strategic learning curves. The histogram shows each participant's correlation between perturbation-driven implicit and strategic learning curves. The vertical dashed line indicates the mean across participants, which is significantly positive. **e**, Perturbation (Pert.)-driven implicit and strategic learning amplitudes across individual participants exhibit a complementary relationship. Each dot depicts an individual participant's implicit (*y* coordinate) and strategic (*x* coordinate) r.m.s. amplitude levels after combining across perturbation-driven frequencies. When perturbation-driven implicit and strategic learning are perfectly aligned with the perturbation, ideal learning would be expected to lie anywhere along the purple dashed line. The data show that the amount of combined learning is very similar across individuals, but the relative contributions of implicit and strategic learning vary widely. **f**, Learning curves of an example participant for perturbation-free frequencies that lie in the range of the perturbation-driven frequencies (1–16 cycles in the training period) for implicit strategic and combined learning. **i**,**k**, Corresponding learning curves for the example participant shown in **f** at medium (17–50 cycles; **i**) and high (51–384 cycles; **k**) frequency ranges in the training period. The data reveal an antagonistic alignment between implicit and strategic components that is strongest at the low frequencies, weaker at medium frequencies and absent at high frequencies. **g**,**j**,**l**, Distribution of correlations between perturbation-free implicit and strategic learning curves. **g**, Histogram of individual participants' correlations between perturbation-free implicit and strategic learning curves, for perturbation-free frequencies that lie in the range of the perturbation-driven frequencies (1–16 cycles in the training period). **j**,**l**, Corresponding histograms for medium (17–50 cycles; **j**) and high (51–384 cycles; **l**) frequency ranges. The thick gray vertical dashed lines indicate the means across participants. Correlations are strongly negative at low frequencies, more weakly negative at medium frequencies and not systematically different from zero at high frequencies. **h**, Perturbation-free implicit and strategic learning amplitudes across individual participants exhibit a closely matched relationship. Each dot depicts an individual participant's implicit (*y* coordinate) and strategic (*x* coordinate) r.m.s. amplitude levels after combining across perturbation-free frequencies that lie in the range of the perturbation-driven frequencies (1–16 cycles in the training period). When perturbation-free implicit and strategic learning are perfectly antagonistically aligned, full cancellation, leading to ideal combined learning, would occur for points that lie along the purple dashed line. This is because oppositely aligned signals can fully cancel one another only when their amplitudes match.

ability of each model to explain the covariance across participants for the r.m.s. perturbation-driven and perturbation-free strategic and implicit learning in our data (Fig. 4).

Noise in motor output is often signal-dependent[31,32], meaning that larger actions lead to larger noise. Since random noise is spread across all frequencies and the number of perturbation-free

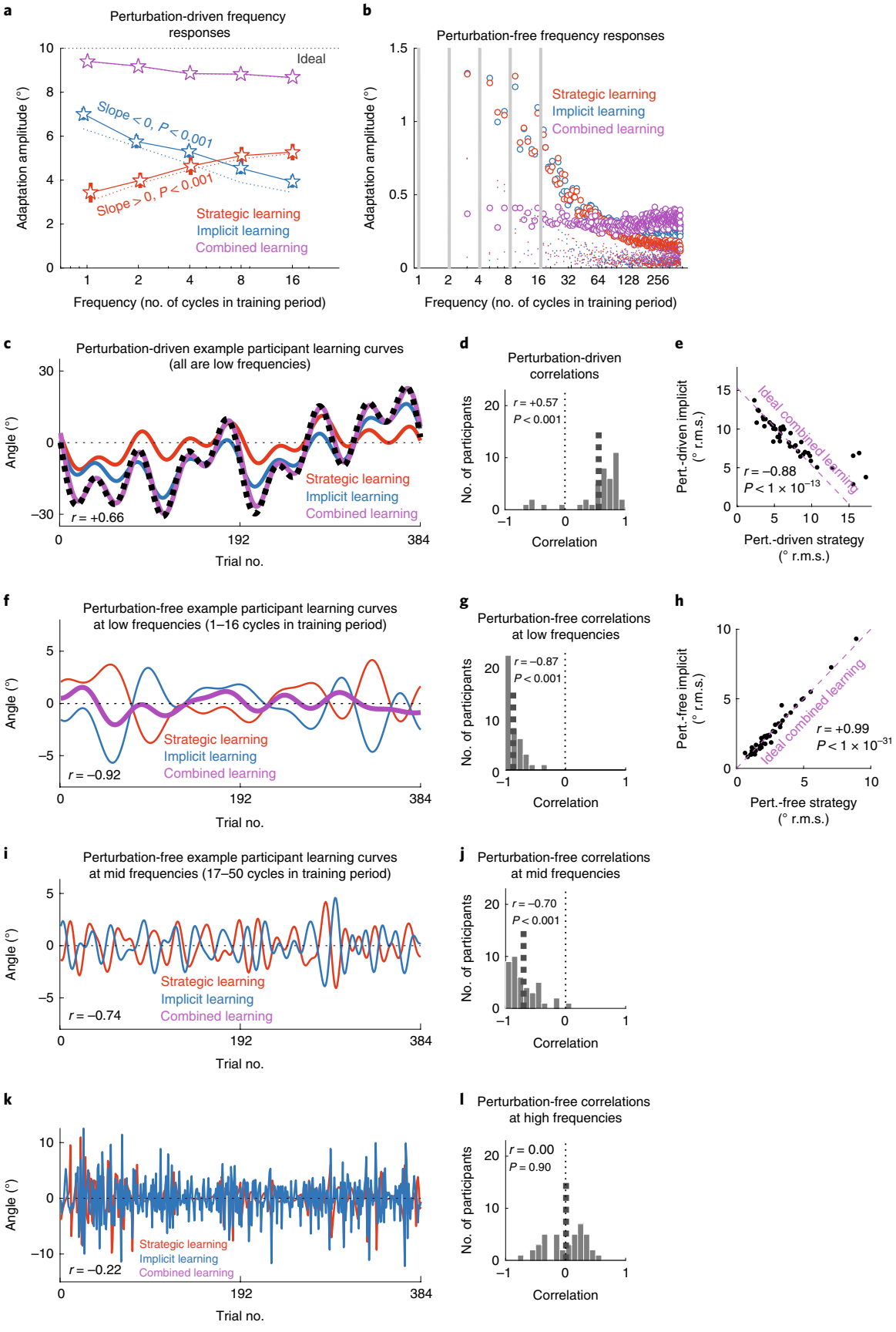

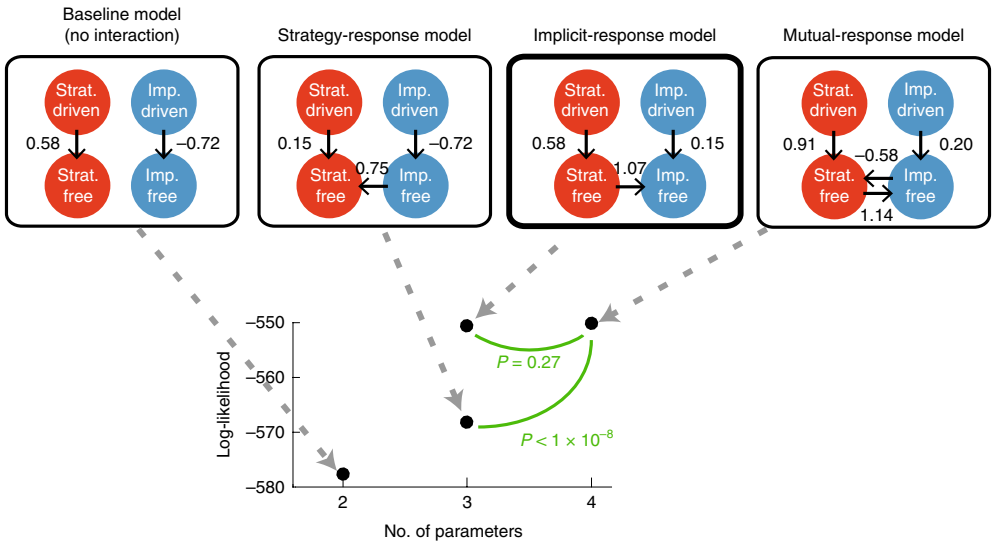

Fig. 4 | SEM analysis of implicit and strategic learning amplitudes shows that implicit learning responds to strategic learning. The different boxes in the top row represent models that hypothesize different interactions between implicit (Imp.) and strategic (Strat.) learning. Arrows indicate the interactions between variables that are posited by the models. The number next to each arrow indicates the strength of the path in the corresponding structural equation model. For each model, we computed the log-likelihood of the fit, plotted in the bottom axis as a function of the number of parameters of the model. The green curves depict nested model comparisons, and the corresponding *P* values reflect the significance of the difference assessed by a likelihood ratio test.

frequencies is much larger than the number of perturbation-driven frequencies (379 versus 5), this random noise would largely reside at perturbation-free frequencies. Thus, the existence of signal-dependent noise would lead to larger perturbation-free responses in participants with larger perturbation-driven adaptive responses, and it is reasonable to think that any nonlinear effects in the adaptive response leading to non-idiosyncratic perturbation-free adaptation would also be larger in individuals with larger perturbation-driven responses. In line with this idea, we constructed a baseline model in which information flow was restricted to be from (1) perturbation-driven to perturbation-free implicit learning and (2) perturbation-driven to perturbation-free strategic learning (Fig. 4, far left). The path strengths in the model shown in Fig. 4 correspond to the amount of information flow inferred by SEM. This baseline model resulted in a path strength of +0.58 from perturbation-driven to perturbation-free strategy and −0.72 from perturbation-driven to perturbation-free implicit learning. The positive path strength between perturbation-driven and perturbation-free strategy indicates that higher levels of perturbation-driven strategy are associated with higher levels of perturbation-free strategy, as expected from signal-dependent noise. However, the negative path strength between perturbation-driven and perturbation-free implicit learning indicates that higher levels of perturbation-driven implicit learning are associated with lower levels of perturbation-free implicit learning. This is opposite to what would be expected from signal-dependent noise, and raises the question of whether perturbation-free implicit adaptation might arise from a mechanism other than the signal-dependent noise captured by this baseline model.

In line with this possibility, we examined three models that build on the baseline model by hypothesizing additional interactions, as illustrated in Fig. 4. In the first of these, perturbation-free strategy responds to perturbation-free implicit learning but not vice versa. This model resulted in a moderate, 9-point log-likelihood ratio compared with the baseline. However, the converse of this model, in which perturbation-free implicit learning responds to perturbation-free strategy but not vice-versa, resulted in a 27-point log-likelihood ratio compared with the baseline. Moreover, it installed a positive path strength for the effect of perturbation-driven on perturbation-free implicit learning, which is in line with the existence of signal-dependent noise. Critically, a mutual-response model, whereby perturbation-free implicit learning responds to perturbation-free strategy and vice versa, also responded to implicit learning and significantly improved on the strategy-response model (log-likelihood ratio = 18.2, $P < 1 \times 10^{-8}$). However, it failed to significantly improve on the implicit-response model (log-likelihood ratio = 0.6, $P = 0.27$), which indicates that while the data provide clear evidence that implicit learning responds to strategy, they fail to provide evidence for an additional effect of strategy responding to implicit learning.

Given that adaptation at perturbation-free frequencies is largely idiosyncratic across individuals, which is in line with it being primarily driven by random sensorimotor noise, the finding that implicit learning actively responds to strategy at these frequencies indicates that it acts to compensate for noise originating from strategy adaptation. If noisy strategy adaptation was the primary driver of perturbation-free adaptive responses, one would expect individuals with higher strategy levels (who should display greater levels of strategy noise) to exhibit systematically worse task performance than low-strategy individuals. This is because effectively compensating for strategy noise would be more challenging in higher strategy individuals. An analysis of the individual differences in task performance revealed that this is indeed the case. We found a positive relationship between overall strategy and task error across all participants across the three experiments ($n = 69$, $t(67) = 6.32$, $P < 1 \times 10^{-5}$), which indicates that participants with larger levels of overall strategy also exhibit larger overall errors. To account for nonspecific effects that might arise from performance differences between experiments, we performed two additional analyses to assess this relationship within just the main experiment ($n = 41$) and with a regression analysis of the full dataset that included experiment as a covariate. In both cases, we again found a significantly positive relationship between strategy use and performance error ($t(39) = 2.38$, $P = 0.01$ for the main experiment data only, and $t(65) = 2.45$, $P < 0.01$ for the combined data). Together, these results indicate that high-strategy participants exhibit systematically larger errors, which is in line with the idea that implicit learning acts to compensate noisy low-fidelity strategy adaptation.

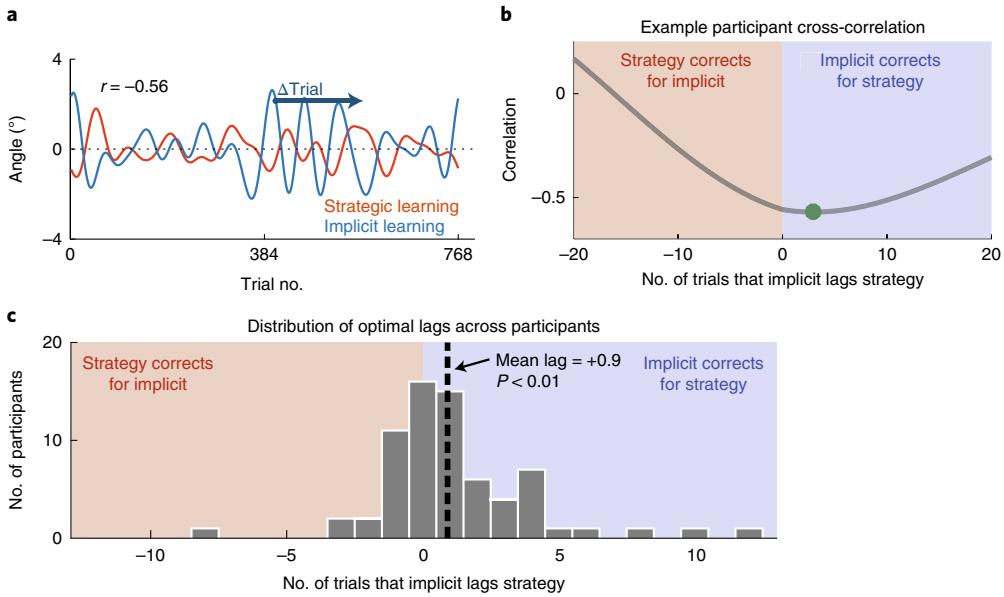

Fig. 5 | An analysis of temporal lags between implicit and strategic learning shows that implicit learning responds to strategic learning. a,**b**, Computing the cross-correlation function between perturbation-free implicit and strategic learning. If one learning process was compensating for the other at low perturbation-free frequencies, its correction would lag behind the process that it is trying to correct. Thus, to find the lag between implicit and strategic perturbation-free learning curves, we shifted the curves relative to each other, as shown for the example participant in **a**, and computed the correlation between the overlapping segments. This results in a cross-correlation function, as shown in **b**, where correlation can be examined as a function of the shift between them (gray curve), allowing us to find the shift with the most negative correlation (green dot), that is, where the correction would be most effective, to estimate the lag between processes. Positive values of the lag (blue shaded area) indicate that implicit learning is lagging behind strategic learning, and negative values of the lag (red shaded area) indicate that strategic learning is lagging behind implicit learning. **c**, Distribution of lags between implicit and strategic learning at perturbation-free frequencies. The histogram shows the distribution of temporal lags for individual participants between perturbation-free implicit and strategic learning curves, based on the cross-correlation function between them. These lags are predominantly positive (blue shaded area), which indicates that perturbation-free implicit learning lags behind strategic learning. The vertical dashed line indicates the mean lag between processes.

Analysis of the temporal lags between implicit and strategic learning indicates that implicit learning compensates for strategy. The SEM analysis was based entirely on data about adaptation amplitudes. To check its robustness, we conducted an independent analysis that was based instead on the temporal lags between perturbation-free implicit and strategic adaptation curves. Because a response must necessarily lag its stimulus, the SEM findings would predict that implicit responses should lag behind strategy at perturbation-free frequencies. If instead, strategy was primarily responding to implicit learning, we would expect strategy to lag behind implicit responses.

We therefore determined the time shift between perturbation-free implicit and strategic learning curves that would maximize antagonistic alignment by finding the shift at which the cross-correlation between these curves was most negative. The data for an example participant shown in Fig. 5a,b displays a maximally antagonistic alignment (that is, maximally negative cross-correlation value) when the implicit learning curve lags behind the strategy learning by three trials (green dot in Fig. 5b), which is in line with implicit learning responding to strategy. Note that the most extreme lags we measured, both positive and negative, correspond to individuals who displayed lower amplitude peak cross-correlations, where it would inherently be more difficult to accurately determine the best alignment. Across all participants, we found maximally antagonistic alignment occurred at $+0.91 \pm 0.34$ trials (Fig. 5c, $P = 0.01$), which suggests that implicit learning systematically lags strategy at the low perturbation-free frequencies where cancellation occurs. The convergent findings of the SEM and time lag analyses, based on the amplitudes and temporal structure of implicit and strategic adaptive responses, point to an implicit learning process that actively responds to compensate low-fidelity explicit strategy.

Simulating interactions between low-fidelity and high-fidelity learning processes reproduces key experimental findings. To ensure that implicit learning effectively responds to noisy strategy learning, it would have to display substantially higher fidelity (that is, lower noise) than strategy learning. Otherwise, the response could do more harm than good. This is the case because the addition of a second adaptive process brings with it not only the adaptive potential to create anticorrelated output capable of canceling the effects of noise from the first process and thus reducing motor error but also its own intrinsic noise that will act to increase error. Thus, effective suppression of error will only occur when the addition of the second process brings with it a noise level that is small enough that the compensation it provides outweighs the noise it adds. A supplementary analysis revealed that at perturbation-free frequencies, net suppression does not occur if the noise level of the second process is higher than that of the first (Extended Data Fig. 1). We therefore wondered whether a difference in fidelity between these learning processes could by itself explain the key interactions between implicit and strategic learning that we described above.

To test this idea, we simulated the interactions between two parallel error-correcting adaptive processes with identical properties except for their fidelity (Fig. 6a; see Methods for equations). In particular, adaptive corrections were corrupted by noise that scaled with the size of the correction, but the scale factor was one-third higher for the high-noise learning process than the low-noise learning process. The high-noise and low-noise processes served as models for strategy and implicit learning, respectively. The sum of these two processes models the combined learning, and the difference between the combined learning and the imposed perturbation is the error signal that drives both adaptive processes. To match the considerable individual differences we observed between the

relative amounts of implicit and strategic learning, we varied the ratio between learning rates for strategy and implicit learning for individual participants ($n = 69$, based on the total size of our dataset) while keeping the mean learning rate across individuals the same for the low-fidelity and high-fidelity processes (Methods). This resulted in a negative correlation between the learning rates for implicit and strategic learning, and while we do not know the mechanism for why this might occur, it appears to be consistent with the data.

Remarkably, this simulation reproduced a number of key features from our experimental data. At perturbation-driven frequencies, the simulated learning displayed synergistic alignment between low-noise and high-noise learning and a complementary relationship between their amplitudes across individuals that echoed experimental observations for implicit and strategic learning (Fig. 6b versus Fig. 3c,d and Fig. 6d upper-left versus Fig. 3e). At perturbation-free frequencies, the simulated processes, similar to the experimental data, exhibited an antagonistic alignment between the learning curves for implicit and strategic learning and closely matched amplitudes of implicit and strategic learning across individuals. This indicates that, as for the experimental data, one adaptive process acts to cancel the inappropriate behavior of the other (Fig. 6c versus Fig. 3f,g and Fig. 6d upper-right versus Fig. 3h). Our simulation also reproduced the results of the SEM analysis (Fig. 6e, and compare with Fig. 4) and the temporal lag analysis (Fig. 6f, and compare with Fig. 5c), which demonstrates that the low-noise process (which models implicit learning) lags behind and effectively compensates for the inappropriate behavior of the high-noise process (which models strategy), a result that can be predicted by mathematical derivation (Supplementary Math Note).

Note that a supplementary analysis (Extended Data Figs. 2–4) revealed that the negative correlation between the learning rates for the implicit and explicit adaptation in the model contributes to the strong correlation between perturbation-driven implicit and strategic learning shown in the upper-left panel of Fig. 6d. However, it does not contribute to the asymmetry in the functional compensation between adaptive processes found in the SEM analysis and lag analysis shown in Fig. 6e,f.

Furthermore, the simulation results, as for the experimental data, displayed a positive relationship between perturbation-free and perturbation-driven amplitude levels for strategic learning, but not for implicit learning (Fig. 6d, lower panels). The positive relationship for strategic learning is expected from signal-dependent noise because inappropriate perturbation-free strategy learning is effectively noise that results from appropriate but imperfect perturbation-driven strategy learning. However, it might be surprising that we did not observe an analogously positive relationship between perturbation-free and perturbation-driven response amplitudes for implicit learning, as signal-dependent noise on implicit learning would, by itself, predict a positive relationship. However, since implicit learning displays low noise and acts to cancel inappropriate strategy at perturbation-free frequencies, most perturbation-free implicit learning comes from compensation for perturbation-free strategy. The compensatory portion of implicit learning at perturbation-free frequencies is inversely correlated with the amplitude of the perturbation-driven implicit learning because low levels of perturbation-driven implicit learning correspond to high levels of perturbation-driven strategy (Fig. 6d, upper left), which results in high levels of perturbation-free strategy (Fig. 6d, lower left) and in turn leading to high levels of compensatory perturbation-free implicit learning (Fig. 6d, upper right). Thus, the difference between the relationships between perturbation-free and perturbation-driven learning for strategy versus implicit adaptation is in line with the idea that perturbation-free strategy is primarily driven by signal-dependent noise for perturbation-driven strategy, whereas perturbation-free implicit learning is largely driven by compensations for perturbation-free strategy.

Overall, the results of this simulation indicate that the key experimental findings illustrated in Figs. 3, 4 and 5 can all be captured by a simple model of two interacting error-correcting processes that differ only in the degree of fidelity, with lower noise characterizing implicit learning and higher noise characterizing strategic learning

Fig. 6 | Model of interactions between low-fidelity and high-fidelity learning processes reproduces key experimental results. a, Illustration of the model. We simulated two error-correcting processes, one with high noise (low-fidelity) and the other with low noise (high-fidelity). The two processes sum to the net motor output and to the error between the net motor output and the perturbation drives each process (see Methods for equations). **b**, The model reproduces synergistic alignment between implicit and strategic learning curves at perturbation-driven frequencies. Left: analogous to Fig. 3c, the data from an example simulated participant show that strategic and implicit learning curves are strongly aligned for perturbation-driven frequencies and synergistically combine to form the combined learning curve. The black dashed line indicates the time course of the ideal learning. Right: analogous to Fig. 3d, the histogram shows each simulated participant's correlation between perturbation-driven implicit and strategic learning curves. The thick vertical dashed line indicates the mean correlation across simulated participants ($r = +0.50$). **c**, The model reproduces antagonistic alignment between implicit and strategic learning curves at perturbation-free frequencies. Left: analogous to Fig. 3f, the data from the same simulated participant as in **b** show that strategic and implicit learning curves are antagonistically aligned for perturbation-free frequencies (in the range of the perturbation-driven frequencies) and largely cancel each other out to form the combined learning curve (purple). Right: analogous to Fig. 3g, the histogram shows each simulated participant's correlation between implicit and strategic learning curves for perturbation-free frequencies (in the range of the perturbation-driven frequencies). The thick vertical dashed line indicates the mean across simulated participants ($r = -0.97$). **d**, The model reproduces inter-individual relationships between perturbation-driven and perturbation-free implicit and strategic learning amplitudes. The upper left and upper right panels are analogous to Fig. 3e,h. Green dots indicate simulated participants, while the black dots indicate participants from the experimental data, showing the participants' r.m.s. amplitude levels after combining across frequencies. The solid lines indicate best fit lines through the correspondingly colored datasets. The dashed purple line indicates the amplitudes that would be expected from ideal combined learning. The model reproduces the complementary relationship between implicit and strategic learning at perturbation-driven frequencies (upper left), the closely matched relationship between implicit and strategic learning at perturbation-free frequencies (upper right), the positive signal-dependent noise relationship between perturbation-free and perturbation-driven strategic learning (lower left) and the negative relationship between perturbation-free and perturbation-driven implicit learning, which suggests that perturbation-free implicit learning is not primarily driven by signal-dependent noise but instead by perturbation-free strategy (lower right). **e**, The model reproduces results of SEM analysis. Analogous to Fig. 4, this panel shows the log-likelihoods for models that hypothesize different interactions between simulated implicit and strategic learning as a function of the number of parameters in the model. The green curves depict nested model comparisons, and the corresponding *P* values reflect the significance of the difference assessed by a likelihood ratio test. **f**, The model reproduces results of the temporal lag analysis. Analogous to Fig. 5c, the histogram shows the distribution of simulated participants' lags between perturbation-free implicit and strategic learning curves, estimated from the cross-correlation function between them. These lags are predominantly positive (blue shaded area), which indicates that the high-fidelity process (model for implicit learning) lags behind the low-fidelity process (model for strategic learning) in the simulation. The vertical dashed line indicates the mean lag between processes.

(Fig. 6). These results are in line with a high-fidelity implicit learning process that compensates for a low-fidelity strategy process during sensorimotor adaptation from one movement to the next. A key general lesson from these modeling results is that a stochastic co-adaptive system with multiple adaptive processes can display emergent dynamics, in which parallel mechanistic responses lead to markedly different functional responses. In particular, we observed that the higher fidelity adaptive component displays robust functional responses to the lower fidelity adaptive component, which arises from mechanistic responses based solely on the overall error. In contrast, the lower-fidelity adaptive component does not display substantial functional responses to the higher-fidelity adaptive component, despite a parallel mechanistic response to the same overall error. This occurs despite the fact that noise output from both adaptive processes directly affects the overall error. The asymmetry of the emergent functional interaction between implicit learning and strategy underscores the dichotomy between functional and mechanistic interactions that can occur in co-adaptive systems, and makes it clear that a computational understanding of adaptive dynamics can add key information to a purely mechanistic description.

Discussion

Here, we uncovered both cooperative and antagonistic interactions between implicit and strategic learning during sensorimotor adaptation using a visuomotor rotation task with a perturbation sequence we designed to separate out adaptive responses into perturbation-driven and perturbation-free dimensions (frequencies). While implicit, strategic and combined learning of the participants readily adapted to perturbations throughout training, these responses were largely concentrated at perturbation-driven frequencies, where we discovered both a cooperative, synergistic alignment between the time courses (Fig. 3c,d) of implicit and strategic learning, and a complementary relationship between their amplitudes (both across frequencies and across individuals; Fig. 3a,e). However, in contrast to the perturbation-driven responses, the perturbation-free responses in the same frequency range displayed an antagonistic relationship

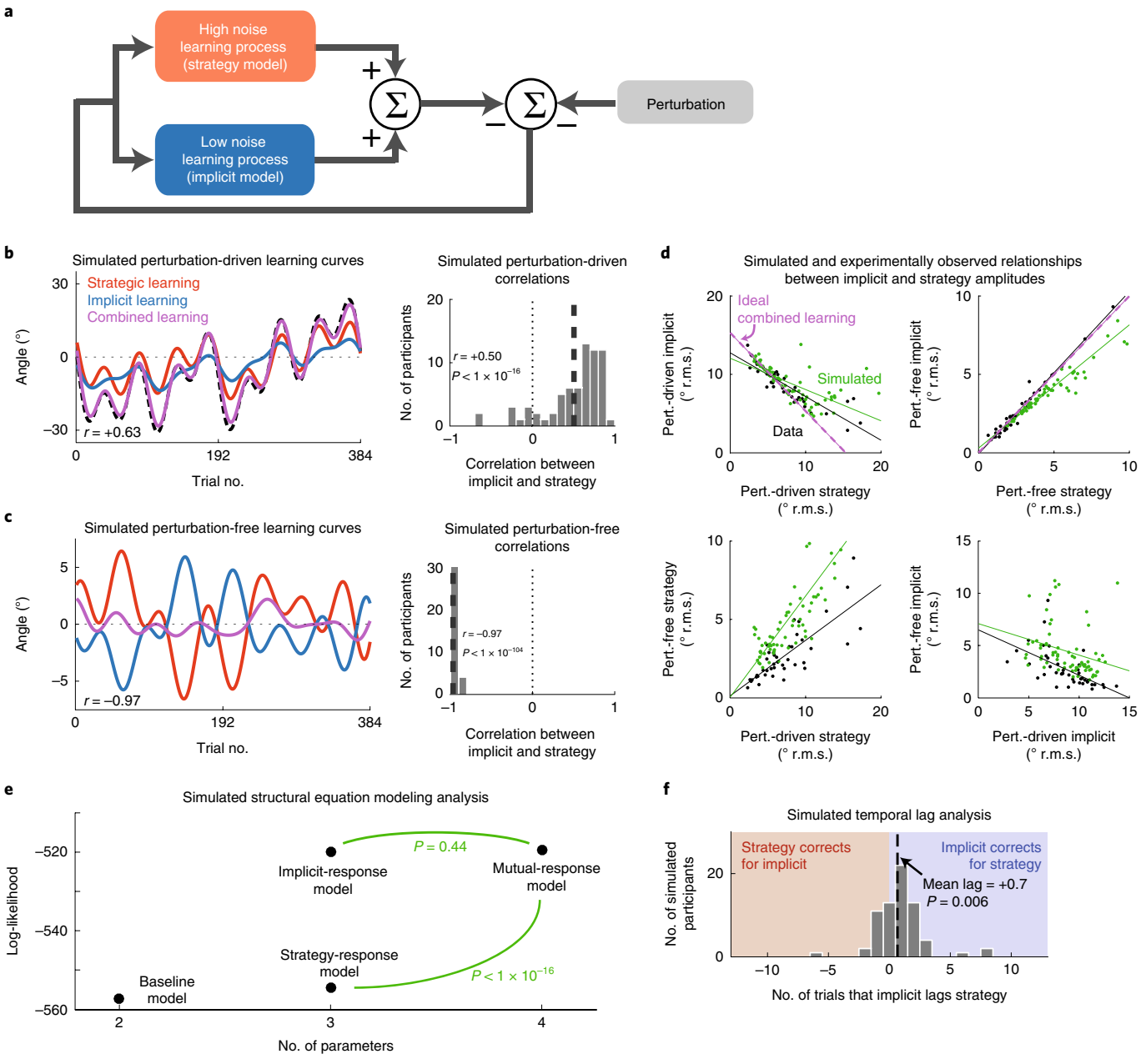

between implicit and strategic learning. Negatively aligned time courses (Fig. 3f,g) and closely matching amplitudes (both across frequencies and across individuals; Fig. 3b,h) together produced highly effective cancellations at these perturbation-free frequencies. These cancellations were particularly effective at lower frequencies (Fig. 3i–l), and resulted from idiosyncratic responses across individuals (Fig. 3b), which suggests that one process actively compensates for noisy inappropriate behavior in the other from trial-to-trial to improve the fidelity of the overall adaptive responses.

To understand whether this trial-to-trial compensation arises from implicit learning compensating for strategic learning or vice versa, we performed two analyses on independent aspects of the data. One investigated the correlation structure in the amplitudes across the adaptive processes in a SEM analysis, independent of temporal information (Fig. 4), and another examined the temporal features of the adaptive processes to determine the time lag of the compensatory behavior, independent of amplitude (Fig. 5). Both found that implicit adaptation responded to explicit strategy rather than the converse, which indicates that implicit learning acts to effectively compensate for inappropriate responses resulting from low-fidelity explicit strategy. Moreover, we demonstrated that a simulation, with two error-correcting processes that differ only in the degree of fidelity, was able to reproduce all key experimental findings (Fig. 6). That is, synergistic interactions at perturbation-driven frequencies, antagonistic interactions at perturbation-free frequencies and effective compensation by the higher fidelity process of inappropriate responses resulting from the lower fidelity process at perturbation-free frequencies. These results indicate that implicit learning takes on a compensatory role in which it effectively cleans up inappropriate responses that can arise from a low-fidelity explicit strategy, providing new insight into the interactions between implicit and explicit processes that occur during learning.

Is implicit learning driven by performance errors or sensory-prediction errors?. Our finding that implicit learning responds to strategy conflicts with the popular theory that implicit learning is driven by sensory-prediction errors and not by performance errors[4,11,33,34]. The performance error associated with an action is the difference between its outcome and the task goal, while the sensory-prediction error is the difference between its outcome and an internal prediction of the outcome. A change in strategy will of course affect the outcome but not the task goal, and thus affect the performance error; however, this change in strategy should affect both the outcome and the internal prediction of the outcome similarly and will therefore have little effect on sensory-prediction error. The fact that we saw implicit learning respond to strategy therefore indicates that implicit learning must respond to performance error, which is at odds with the claim that implicit learning is driven by sensory-prediction errors but not by performance errors.

Meanwhile, the claim that implicit learning is driven by sensory-prediction errors and not by performance errors is based on the conclusion by Mazzoni and Krakauer in 2006 (ref. [6]) that implicit adaptation proceeds independently of strategy, and by Krakauer in 2009 (ref. [11]), which later interpreted this independence to mean that implicit adaptation is purely driven by sensory prediction errors rather than performance errors. Specifically, the idea that implicit learning is driven by sensory-prediction error is based on the finding that it can proceed even when performance error is eliminated by the use of experimentally prescribed strategies[6]. This finding indicates that sensory-prediction error contributes to implicit adaptation; however, it does not indicate that sensory-prediction error is the sole driver of implicit adaptation.

To show that sensory-prediction error is the sole driver of implicit adaptation (that is, that implicit learning proceeds independently of performance error and strategy), one must show that implicit adaptation identically proceeds when performance error is present or absent. Indeed, Mazzoni and Krakauer[6] argued for identical adaptation; however, this claim relied on a negative result for which the evidence was weak. They found that a non-strategy condition, which allowed performance errors, displayed initial learning that was nominally faster than that of the strategy condition, which eliminated them (34.9% versus 30.4%), which is actually in line with performance-error-driven learning. The difference was not significant ($P=0.223$) and was consistent with identical adaptation, but the data were also consistent with a 95% confidence interval that included a 25% higher initial learning rate for the non-strategy group, thereby indicating poor statistical power. Moreover, late learning was substantially and significantly larger for the non-strategy group than the strategy group (65% difference with $P<0.005$), with a 95% confidence interval that included a 100% higher initial learning rate for the non-strategy group. The authors suggested that the large difference they observed in late learning might be due to participants altering their strategies late in training; however, strategy levels were not measured in these participants. Thus, the initial learning rate results are consistent with the absence of performance-error-driven implicit learning and are consistent with performance-error-driven implicit learning that is 25% as high as sensory-prediction error-driven implicit learning, and the final adaptation results are consistent with performance-error-driven implicit learning that could, in fact, be as large or larger than sensory-prediction error-driven implicit learning. This suggests that implicit learning may be driven, at least in part, by performance errors, which is consistent with our findings that implicit learning can respond to strategy and in line with previous studies that showed that strategy use interferes with the build-up of implicit adaptation[8,26], as strategy use would decrease the performance errors that could drive implicit adaptation.

A number of recent studies have presented converging evidence that points to multiple adaptive processes that contribute to motor adaptation[18,35,36]. Although little is known about the specific error signals that drive these different processes, an intriguing possibility is that distinct components of implicit learning are driven by performance errors and sensory-prediction errors.

Interference between explicit and implicit processes in motor skill learning. An important idea in motor skill learning research is that motor learning proceeds from predominantly explicit to implicit states as a learner develops from novice to expert[37,38]. Interestingly, instructing subjects to verbalize or monitor their actions to promote the use of explicit strategies improves performance at novice stages, at which learning is largely explicit, but impairs performance at expert stages, at which learning is primarily implicit[39–42]. That novice performance is improved is in line with our results and other work showing that strategy is capable of rapid learning[4,9] and able to adapt to rapidly changing, high-frequency perturbations (Fig. 3a), which are helpful during initial stages of learning where overall performance is far from the ideal level. Strategy may also be useful in adapting to complex, but cognitively predictable perturbation patterns. However, that expert performance is impaired is in line with our current results showing that strategy, with its low fidelity, is more susceptible to noise. This can make the overuse of strategy detrimental during late stages of learning, where overall performance is appropriately centered and achieving precision is the dominant factor, because the use of a low-fidelity strategy reduces precision.

Interestingly, the impairment observed at expert stages occurs not only when performance is tested concurrently during the verbalization[39–41] but also when tested subsequently without verbalization[42]. This persistent effect suggests that promoting explicit strategies may interfere with the development of implicit motor learning. In line with this idea, some motor adaptation studies have found that implicit learning is attenuated by the use of explicit strategies[8,26]. In the current study, we found that implicit learning

is attenuated by explicit strategy on an individual participant level, with a strong negative inter-individual correlation between the amounts of implicit learning and strategic learning at perturbation-driven frequencies (Fig. 3e, $r=-0.88$), which means that individuals with higher perturbation-driven implicit learning display systematically lower levels of strategic learning and vice versa. These behavioral findings are consistent with other work showing that the neural systems underlying explicit and implicit processes may competitively interact[43,44]; for example, lesions to medial temporal lobe structures, which support explicit declarative memory, can in fact improve implicit procedural learning[43–45], which largely depends on other brain regions, including the basal ganglia, motor cortical areas and the cerebellum[17,35,43,44,46–50]. The current study extends the current understanding of the interference between explicit and implicit processes in motor learning by showing that high noise in explicit strategy is systematically compensated for by adaptive changes in implicit learning to improve the reliability of the overall motor output.

Online content

Any methods, additional references, Nature Research reporting summaries, source data, extended data, supplementary information, acknowledgements, peer review information; details of author contributions and competing interests; and statements of data and code availability are available at https://doi.org/10.1038/s41593-020-0600-3.

Received: 22 May 2017; Accepted: 28 January 2020;
Published online: 28 February 2020

References

1. Ellis, N. Rules and instances in foreign language learning: interactions of explicit and implicit knowledge. *Eur. J. Cogn. Psychol.* **5**, 289–318 (1993).
2. Gugerty, L. J. Situation awareness during driving: explicit and implicit knowledge in dynamic spatial memory. *J. Exp. Psychol. Appl.* **3**, 42–66 (1997).
3. Schendan, H. E., Searl, M. M., Melrose, R. J. & Stern, C. E. An fMRI study of the role of the medial temporal lobe in implicit and explicit sequence learning. *Neuron* **37**, 1013–1025 (2003).
4. Taylor, J. A., Krakauer, J. W. & Ivry, R. B. Explicit and implicit contributions to learning in a sensorimotor adaptation task. *J. Neurosci.* **34**, 3023–3032 (2014).
5. Kahneman, D. & Egan, P. *Thinking, Fast and Slow* Vol. 1 (Farrar, Straus and Giroux New York, 2011).
6. Mazzoni, P. & Krakauer, J. W. An implicit plan overrides an explicit strategy during visuomotor adaptation. *J. Neurosci.* **26**, 3642–3645 (2006).
7. Taylor, J. A., Klemfuss, N. M. & Ivry, R. B. An explicit strategy prevails when the cerebellum fails to compute movement errors. *Cerebellum* **9**, 580–586 (2010).
8. Benson, B. L., Anguera, J. A. & Seidler, R. D. A spatial explicit strategy reduces error but interferes with sensorimotor adaptation. *J. Neurophysiol.* **105**, 2843–2851 (2011).
9. Bond, K. M. & Taylor, J. A. Flexible explicit but rigid implicit learning in a visuomotor adaptation task. *J. Neurophysiol.* **113**, 3836–3849 (2015).
10. Krakauer, J. W., Pine, Z. M., Ghilardi, M.-F. & Ghez, C. Learning of visuomotor transformations for vectorial planning of reaching trajectories. *J. Neurosci.* **20**, 8916–8924 (2000).
11. Krakauer, J. W. in *Progress in Motor Control* Vol. 629 (ed. Sternad, D.) 405–421 (Springer US, 2009).
12. Brayanov, J. B., Press, D. Z. & Smith, M. A. Motor memory is encoded as a gain-field combination of intrinsic and extrinsic action representations. *J. Neurosci.* **32**, 14951–14965 (2012).
13. Wu, H. G. & Smith, M. A. The generalization of visuomotor learning to untrained movements and movement sequences based on movement vector and goal location remapping. *J. Neurosci.* **33**, 10772–10789 (2013).
14. Von Helmholtz, H. *Handbuch der Physiologischen Optik* Vol. 9 (Voss, 1867).
15. Held, R. & Freedman, S. J. Plasticity in human sensorimotor control. *Science* **142**, 455–462 (1963).
16. Shadmehr, R. & Mussa-Ivaldi, F. A. Adaptive representation of dynamics during learning of a motor task. *J. Neurosci.* **14**, 3208–3224 (1994).
17. Smith, M. A. & Shadmehr, R. Intact ability to learn internal models of arm dynamics in Huntington's disease but not cerebellar degeneration. *J. Neurophysiol.* **93**, 2809–2821 (2005).
18. Smith, M. A., Ghazizadeh, A. & Shadmehr, R. Interacting adaptive processes with different timescales underlie short-term motor learning. *PLoS Biol.* **4**, e179 (2006).
19. Joiner, W. M. & Smith, M. A. Long-term retention explained by a model of short-term learning in the adaptive control of reaching. *J. Neurophysiol.* **100**, 2948–2955 (2008).
20. Wagner, M. J. & Smith, M. A. Shared internal models for feedforward and feedback control. *J. Neurosci.* **28**, 10663–10673 (2008).
21. Sing, G. C., Joiner, W. M., Nanayakkara, T., Brayanov, J. B. & Smith, M. A. Primitives for motor adaptation reflect correlated neural tuning to position and velocity. *Neuron* **64**, 575–589 (2009).
22. Kagerer, F. A., Contreras-Vidal, J. L. & Stelmach, G. E. Adaptation to gradual as compared with sudden visuo-motor distortions. *Exp. Brain Res.* **115**, 557–561 (1997).
23. Taylor, J. A., Wojaczynski, G. J. & Ivry, R. B. Trial-by-trial analysis of intermanual transfer during visuomotor adaptation. *J. Neurophysiol.* **106**, 3157–3172 (2011).
24. Alhussein, L., Hosseini, E. A., Nguyen, K. P., Smith, M. A. & Joiner, W. M. Dissociating effects of error size, training duration, and amount of adaptation on the ability to retain motor memories. *J. Neurophysiol.* **122**, 2027–2042 (2019).
25. Taylor, J. A. & Ivry, R. B. Flexible cognitive strategies during motor learning. *PLoS Comput. Biol.* **7**, e1001096 (2011).
26. Jakobson, L. S. & Goodale, M. A. Trajectories of reaches to prismatically-displaced targets: evidence for 'automatic' visuomotor recalibration. *Exp. Brain Res.* **78**, 575–587 (1989).
27. Hudson, T. E. & Landy, M. S. Measuring adaptation with a sinusoidal perturbation function. *J. Neurosci. Methods* **208**, 48–58 (2012).
28. Kettner, R. E. et al. Prediction of complex two-dimensional trajectories by a cerebellar model of smooth pursuit eye movement. *J. Neurophysiol.* **77**, 2115–2130 (1997).
29. Stein, C. M., Morris, N. J. & Nock, N. L. Structural equation modeling. *Methods Mol. Biol.* **850**, 495–512 (2017).
30. de Marco, G. et al. Principle of structural equation modeling for exploring functional interactivity within a putative network of interconnected brain areas. *Magn. Reson. Imaging* **27**, 1–12 (2009).
31. Harris, C. M. & Wolpert, D. M. Signal-dependent noise determines motor planning. *Nature* **394**, 780–784 (1998).
32. Jones, K. E., Hamilton, A. F. C. & Wolpert, D. M. Sources of signal-dependent noise during isometric force production. *J. Neurophysiol.* **88**, 1533–1544 (2002).
33. Shadmehr, R., Smith, M. A. & Krakauer, J. W. Error correction, sensory prediction, and adaptation in motor control. *Annu. Rev. Neurosci.* **33**, 89–108 (2010).
34. Krakauer, J. W. & Mazzoni, P. Human sensorimotor learning: adaptation, skill, and beyond. *Curr. Opin. Neurobiol.* **21**, 636–644 (2011).
35. Hadjiosif, A. et al. Cerebellar damage reduces the stability of motor memories. in *Proc. Transl. Comput. Mot. Control* https://sites.google.com/site/acmcconference/2014/30.pdf (2014).
36. Haith, A. M., Huberdeau, D. M. & Krakauer, J. W. The influence of movement preparation time on the expression of visuomotor learning and savings. *J. Neurosci.* **35**, 5109–5117 (2015).
37. Fitts, P. M. & Posner, M. I. *Human Performance* (Brooks/Cole, 1967).
38. Anderson, J. R. Acquisition of cognitive skill. *Psychol. Rev.* **89**, 369–406 (1982).
39. Beilock, S. L., Wierenga, S. A. & Carr, T. H. Expertise, attention, and memory in sensorimotor skill execution: impact of novel task constraints on dual-task performance and episodic memory. *Q. J. Exp. Psychol. Sect. A* **55**, 1211–1240 (2002).
40. Gray, R. Attending to the execution of a complex sensorimotor skill: expertise differences, choking, and slumps. *J. Exp. Psychol. Appl.* **10**, 42–54 (2004).
41. Jackson, R. C., Ashford, K. J. & Norsworthy, G. Attentional focus, dispositional reinvestment, and skilled motor performance under pressure. *J. Sport Exerc. Psychol.* **28**, 49–68 (2006).
42. Flegal, K. E. & Anderson, M. C. Overthinking skilled motor performance: or why those who teach can't do. *Psychon. Bull. Rev.* **15**, 927–932 (2008).
43. Poldrack, R. A. et al. Interactive memory systems in the human brain. *Nature* **414**, 546–550 (2001).
44. Poldrack, R. A. & Packard, M. G. Competition among multiple memory systems: converging evidence from animal and human brain studies. *Neuropsychologia* **41**, 245–251 (2003).
45. Packard, M. G., Hirsh, R. & White, N. M. Differential effects of fornix and caudate nucleus lesions on two radial maze tasks: evidence for multiple memory systems. *J. Neurosci.* **9**, 1465–1472 (1989).
46. Boyd, L. A. & Winstein, C. J. Providing explicit information disrupts implicit motor learning after basal ganglia stroke. *Learn. Mem.* **11**, 388–396 (2004).
47. Karni, A. et al. The acquisition of skilled motor performance: fast and slow experience-driven changes in primary motor cortex. *Proc. Natl Acad. Sci. USA* **95**, 861–868 (1998).

48. Martin, T. A., Keating, J. G., Goodkin, H. P., Bastian, A. J. & Thach, W. T. Throwing while looking through prisms: I. Focal olivocerebellar lesions impair adaptation. *Brain* **119**, 1183–1198 (1996).
49. Diedrichsen, J., Verstynen, T., Lehman, S. L. & Ivry, R. B. Cerebellar involvement in anticipating the consequences of self-produced actions during bimanual movements. *J. Neurophysiol.* **93**, 801–812 (2005).
50. Breska, A. & Ivry, R. B. Double dissociation of single-interval and rhythmic temporal prediction in cerebellar degeneration and Parkinson's disease. *Proc. Natl Acad. Sci. USA* **115**, 12283–12288 (2018).

Methods

Participants. A total of 41 participants (30 female, 35 right-handed, mean age 21.7 years) took part in the main sum-of-sines visuomotor rotation experiment, in which the visuomotor rotation sequence was composed of sinusoids at 5 different frequencies (Fig. 2). A total of 14 participants (11 female, 10 right-handed, mean age 22 years) took part in the additional seven-frequency sum-of-sines visuomotor rotation experiment, and another 14 participants (8 female, 12 right-handed, mean age 23.9 years) took part in the additional four-frequency sum-of-sines visuomotor rotation experiment. Participants were naive to the purpose of the experiments, had no known neurological conditions and gave written informed consent, consistent with the policies of the Institutional Review Board for Harvard University. No statistical methods were used to predetermine sample sizes, but the sample sizes we used were similar to or greater than those reported in previous publications[4,6–27].

Apparatus. Participants sat facing a 120-Hz, 23-inch LCD monitor, mounted horizontally at shoulder level, that displayed visual cues during the experiment. The latency of real-time visual feedback was 23–25 ms based on an analysis of 240 fps external video recordings that simultaneously captured hand motion and visual feedback on the screen. Underneath this monitor and hidden from their view, participants grasped a foam handle (cylindrical, 25 mm in diameter) that encased a digital stylus, and performed movements by sliding it atop a digitizing tablet (Wacom Intuos 3) that recorded hand position at 200 Hz with 0.005-mm resolution. The bottom of the foam handle was lined with Teflon tape to allow it to slide smoothly over the tablet surface. Participants were positioned such that their midlines were aligned with the middle of the monitor and tablet surface. Software for running the experiment was designed using Psychophysics Toolbox 3.0 in Matlab R2010a.

Experimental protocol. *Targets and cursor feedback.* Participants performed rapid 9-cm point-to-point reaching arm movements with their dominant hands toward different targets, executed at peak speeds of 37.2 ± 10.1 cm s^{-1} (mean ± s.d. across participants). The starting location for each reaching movement was shown as a circle with a diameter of 5 mm labeled with a 'S' (which stood for Start), and each target was a circle 10 mm in diameter. In addition, cursor feedback of hand location, when provided, was displayed as a circle 2.5 mm in diameter.

Aiming marker. During the training period and later parts of the baseline period, participants were told that the cursor they were attempting to move to the target might be skewed from their hand direction and that aiming at a position distinct from the target might sometimes improve performance. Moreover, they were told that the amount of skew might change from one trial to the next so that the aiming point that would be most beneficial might also change from one trial to the next. To help visualize an aim point for the reaching movement, participants were provided with a marker, displayed as a 10-mm diameter red ring. This aiming marker was positioned by the experimenter during earlier parts of the baseline period, but was positioned by the participant during the training period and the last block of the baseline period. The aiming marker could be positioned in any direction but was constrained to be the same distance away from the starting location as the target. Participants positioned the aiming marker by pressing the left and right arrow keys multiple times on a keypad using the non-reaching hand, and then registered the chosen aim point by pressing the up arrow key. This aiming procedure occurred before the required reaching movement.

Baseline period. The experiment started with the baseline period, which consisted of three types of baseline blocks. The first was a familiarization baseline block, which familiarized participants with the basic experimental setup and target-reaching task. This block consisted of 50 trials and presented participants with no aiming marker and only the starting location, target and cursor, which presented veridical feedback of hand position. In this block, the target was always presented at the 0° direction (upward).

The familiarization baseline block was followed by two fixed-aiming baseline blocks, each comprising 50 trials. In these fixed-aiming baseline blocks, participants were presented not only with the starting location, target and cursor but also with an aiming marker. The position of this aiming marker was fixed and predetermined by the experimenters. These blocks familiarized participants with the presence of an aiming marker and the procedure of aiming for it. Here, targets appeared at different directions for each trial, from −90° and 90°, every 30°. For the majority of trials in these blocks, participants were presented with cursor feedback that veridically displayed hand position, and the aiming marker was placed directly on top of the target during these trials to facilitate accurate cursor motion toward the target. However, on occasional trials (1 every 5), cursor feedback of the hand direction was rotated by 30° (50% of these trials in the clockwise direction and 50% in the counter-clockwise direction for each participant, presented in random order). For these trials, the aiming marker was correspondingly displaced from the target location by 30°, such that aiming for the aiming marker would facilitate accurate cursor movement toward the target on these trials as well. Thus, these rotation trials familiarized participants with the procedure of aiming for an aiming marker even when it does not overlap with the target. Note that any learning resulting from these isolated rotation trials were immediately washed away by many non-rotation trials following it.

The baseline period concluded with a variable-aiming baseline block of 50 trials that familiarized participants with the procedure of aiming for an aiming marker that they positioned themselves. The cursor veridically displayed hand position on these trials. As for the previous block, targets appeared at different directions for each trial, from −90° and 90° every 30°; however, the position of the aiming marker was not fixed and could be adjusted by the participant using arrow keys that the participants manipulated with the non-reaching hand.

Training periods. In the training period, participants were presented with a single target direction at 0° (upward). This period started with 50 trials for which the visuomotor rotation was 0° (displaying veridical hand position), followed by trials for which the visuomotor rotation changed according to a sequence that was constructed using sinusoid components (Fig. 1b). In the main experiment, we constructed this rotation sequence using 5 pure sine wave components with 10° amplitudes and periods of 48, 96, 192, 384 and 768 trials, as shown by the black dashed line in Fig. 2a. These periods correspond to frequencies of 16, 8, 4 and 2 cycles and 1 cycle, respectively, in the training period (black dashed line in Fig. 2b), where the training period was 768-trials long. Using pure sine waves avoids a discontinuity at perturbation sequence onset. The two additional experiments used rotation sequences composed of 7 sine components with 10° amplitudes and periods of 6, 12, 24, 48, 96, 192, 384 trials (which correspond to 128, 64, 32, 16, 8, 4 and 2 cycles, respectively, in 768 trials of training) and 4 sine components with 10° amplitudes and periods of 48, 96, 192 and 384 trials (which correspond to 8, 4 and 2 cycles and 1 cycle, respectively, in 384 trials of training). To eliminate the possible effects of being trained on a positive versus negative version of the visuomotor rotation sequence, these conditions were balanced across participants. A total of 20 versus 21 participants were trained on the positive versus negative version of the sequence, respectively, for the five-frequency experiment, 7 versus 7 participants for the seven-frequency experiment, and 7 versus 7 participants for the four-frequency experiment.

Analysis. *Calculating hand direction.* The data presented were taken from outward movements initiated from the center starting location; return movements back to the center were not analyzed. For each movement, we calculated the hand direction as the direction of the hand when it was 6 cm away from the starting location compared with its position when 2 cm away. The 2 cm and 6 cm points occurred at 85.5 ± 22.9 ms and 166.6 ± 59.5 ms, respectively, (mean ± s.d. across participants) after movement onset, defined as the time at which hand speed first exceeded 6.35 cm s^{-1}. The hand speeds at the 2 cm and 6 cm locations were 47.4 ± 16.3 cm s^{-1} and 55.8 ± 21.4 cm s^{-1}, respectively.

Calculating strategy, implicit learning and combined learning. For each trial, strategy was calculated as the difference between the aiming direction, as indicated by the angle of the aiming marker (red dashed line in Fig. 1a) and the cursor target direction (black dashed line in Fig. 1a). Implicit learning was calculated as the difference between the hand motion direction (purple arrow in Fig. 1a) and the aiming direction. Combined learning was the sum of strategy and implicit learning and amounted to the difference between the hand motion direction and cursor target direction.

Outlier analysis. No participants were excluded from the dataset. Individual trials were excluded as outliers if the product of consecutive differences in strategy were greater than 4,000 degrees^2 in magnitude. This resulted in the omission of <0.1% of trials (19 out of 47,616).

Frequency-based analysis of adaptation. To represent the perturbation sequence and the learning curves for implicit, strategic and combined adaptation as a function of amplitude at different frequencies, we regressed these data onto sinusoids at each frequency up to the Nyquist limit (half the total number of trials). This allowed us to represent the perturbation sequence, implicit, strategic and combined learning curves as a function of amplitude and phase at different frequencies, as shown in Figs. 2b,d and 3a,b.

Note that the DC offset (frequency = 0) components of adaptation are not shown in Figs. 2 and 3; however, like the other perturbation-free frequencies, the DC offset also showed an antagonistic interaction and closely matched amplitudes between implicit and strategic learning. Because a DC offset does not change around its mean, the correlation coefficient between implicit and strategic learning time courses for the DC offset is undefined and thus cannot characterize their relationship. However, we can compute the correlation between the sign of the implicit DC offset and the sign of the strategic DC offset across individual participants as an analogous measure. In doing so, we found that the signs of the DC offset were strongly negatively correlated ($r = -0.67$, $F(1, 41) = 30.9$, $P < 1 \times 10^{-5}$ for the main five-frequency experiment), which indicates an antagonistic relationship. Furthermore, the amplitudes of the DC offset were strongly positively correlated across individual participants ($r = 0.93$, $F(1, 41) = 266$, $P < 1 \times 10^{-18}$ for the main five-frequency experiment), which indicates a close match in the amplitudes of the implicit and strategic DC offsets, analogous to

the results shown in Fig. 3h. The additional seven-frequency and four-frequency experiments showed consistent trends, but with weaker statistical power ($r=-0.29$, $F(1, 14)=1.09$, $P=0.32$ for the seven-frequency experiment signs, and $r=-0.34$, $F(1, 14)=1.54$, $P=0.24$ for the four-frequency experiment signs; $r=0.98$, $F(1, 14)=227$, $P<1\times10^{-8}$ for the seven-frequency experiment amplitudes, and $r=0.89$, $F(1, 14)=43.9$, $P<1\times10^{-4}$ for the four-frequency experiment amplitudes), and this is consistent with the smaller size of their datasets.

SEM analysis on implicit and strategic learning amplitudes. To analyze whether information flows from implicit learning to strategic learning versus from strategic learning to implicit learning, we conducted a SEM analysis on the amplitudes of perturbation-driven and perturbation-free implicit and strategic learning. This analysis compared different models of how information flows between multiple key variables of interest, where the parameters of the model corresponded to the strengths of the directional flows between variables, and the model was fit by minimizing the difference between observed and model-predicted covariance structures via maximum likelihood[51,52]. These models were fit using the sem function in the Lavaan package for R[53]. The strengths of the directional flows between variables (path coefficients) represent the response of the dependent variable to a unit change in an explanatory variable, while accounting for the other variables. We used a likelihood ratio test to test for a significant difference in likelihood between nested models; details are noted in the "Statistical tests" section below.

Analyzing the relationship between error and strategy levels. To increase the statistical power in our ability to analyze the relationship between error and strategy levels, we combined data from participants across three experiments (the main five-frequency experiment, along with an additional four-frequency experiment and seven-frequency experiment). In this analysis, we computed the r.m.s. levels of error and strategy for each participant and determined whether the effect of strategy was significantly positive when regressing error level onto strategy level. Since the four-frequency experiment was run only for 384 trials, we used the first 384 out of the 768 trials for the five-frequency and seven-frequency experiments to match the trial numbers across the different experiments calculated. To assess this relationship between error and strategy while accounting for systematic mean differences across the three experiments, we performed two additional regression analyses: one in which we examined only the data from the main experiment ($n=41$) and one in which we combined the data across experiments ($n=69$), but included experiment as a covariate while assessing the significance of strategy level.

Temporal lag analysis of implicit and strategic learning time courses. To understand whether implicit learning corrections lag behind strategic learning or strategic learning corrections lag behind implicit learning at the low perturbation-free frequencies, we performed an analysis of their temporal lags. For each participant, we computed the cross-correlation function between implicit and strategy learning curves at the low-frequency perturbation-free frequencies by shifting the curves relative to each other at different lags (Fig. 5a) and calculating the correlation between the overlapping segments. We then examined each participant's cross-correlation function to find the lag at which the correlation was most negative (Fig. 5b); that is, where the cancellation due to the antagonistic correction would be most effective. These optimal lags are shown in the histogram in Fig. 5c.

Simulation of interactions between low-noise and high-noise learning processes. To understand whether a difference in noise-levels (fidelity) between implicit (I) and strategic (S) learning could explain the interactions between implicit and strategic learning (as shown in Figs. 3, 4 and 5), we simulated two parallel error-correcting adaptive processes (Fig. 6a) with identical properties except for their noise levels.

This simulation is described by the equations below:

$$x_S(n+1) = A_S x_S(n) + B_S e(n) + \epsilon_S(n+1)$$

$$x_I(n+1) = A_I x_I(n) + B_I e(n) + \epsilon_I(n+1)$$

$$x_{comb}(n+1) = x_S(n+1) + x_I(n+1) + \epsilon_{out}(n+1)$$

$$e(n+1) = P(n+1) - x_{comb}(n+1)$$

where $x_S(n)$ and $x_I(n)$ represent the states of the processes at trial n, A_S and A_I represent their retention factors, B_S and B_I represent their learning rates, and $\varepsilon_S(n)$ and $\varepsilon_I(n)$ represent Gaussian noise that corrupts their states. $x_{comb}(n)$ represents the combined output, which is corrupted by Gaussian noise, $\varepsilon_{out}(n)$, $P(n)$ represents the perturbation, and $e(n)$ represents the error between them, which drives the individual processes.

The noise components $\varepsilon_S(n)$, $\varepsilon_I(n)$ and $\varepsilon_{out}(n)$ are defined as follows:

$$\epsilon_S(n) \sim N(0, k_S B_S e(n))$$

$$\epsilon_I(n) \sim N(0, k_I B_I e(n))$$

$$\epsilon_{out}(n) \sim N(0, \sigma)$$

The sizes of ε_S and ε_I scale with the sizes of the corrections made by the processes ($k_S B_S e(n)$, $k_I B_I e(n)$). The scaling factor for each adaptive process (k_S, k_I) distinguishes the noise levels (fidelity) between the processes, and is the only feature that is asymmetric between these processes: 33% higher for one than the other ($k_S=2.0$, $k_I=1.5$). The size of the output noise (σ) was set to be 2.

To simulate individual differences in strategic and implicit learning amplitudes (we simulated $n=69$, based on the total size of our dataset), we uniformly varied the learning rates of the two processes around a mean learning rate ($B=0.34$) according to the following equations:

$$\theta_i \sim \text{Unif}(-c, c)$$

$$B_{S_i} = B + \theta_i$$

$$B_{I_i} = B - \theta_i$$

Thus, the learning rate for one process was varied according to a uniform distribution ($c=0.16$) centered around a mean learning rate ($B=0.34$), and the corresponding learning rate for the other process was varied in a complementary fashion. Note that varying the learning rates in this way does not introduce any systematic differences in learning rate between the two simulated processes. The retention factor was kept the same between both processes and across individuals ($A_S=A_I=0.9$).

Statistical tests. The data distribution was assumed to be normal unless otherwise indicated below, but this was not formally tested. Paired t-tests were used for the following comparisons: (1) perturbation-driven amplitudes versus perturbation-free amplitudes (two-sided) for implicit, strategic and combined learning, where amplitudes were averaged across perturbation-driven frequencies for each participant and across perturbation-free frequencies for each participant (Fig. 2b,d); (2) combined versus implicit and strategy perturbation-driven amplitudes (two-sided), where amplitudes were averaged across perturbation-driven frequencies for each participant (Fig. 3a); and (3) combined versus implicit and strategy perturbation-free amplitudes (two-sided), where amplitudes were averaged across perturbation-driven frequencies for each participant (Fig. 3b). One-sample t-tests were used to test the following comparisons: (1) whether the correlation between implicit and strategic learning across their time courses, calculated for each participant, is different from zero (two-sided) across participants for perturbation-driven frequencies (Fig. 3d) and for perturbation-free frequencies (Fig. 3g,j,l); (2) whether the slope of amplitude versus frequency across perturbation-driven frequencies, calculated for each participant, is different from zero (two-sided) across participants for implicit and strategic learning (Fig. 3a); (3) whether the correlation between implicit and strategic learning amplitudes across low perturbation-free frequencies (1–16 cycles), calculated for each participant, is different from zero (two-sided) across participants (Fig. 3b); and (4) whether the relationship between error and strategy levels is significantly positive (one-sided). F-tests were used for the following comparisons: (1) whether the correlation between implicit and strategic r.m.s. amplitudes across individual participants is different from zero for perturbation-driven frequencies (Fig. 3e) and for low perturbation-free frequencies (1–16 cycles, Fig. 3h); and (2) whether the correlation between signs of implicit and strategic DC offsets across individual participants and between amplitudes of implicit and strategic DC offsets across individual participants is different from zero. A likelihood ratio test was used to compare the likelihoods across nested models in the SEM analysis (Fig. 4). In particular, we computed the likelihood ratio test statistic (Λ), that is, the ratio of likelihoods between two nested models, where the numerator represents the simpler of the two models. Under the null hypothesis (that the parameters are constrained, as represented by the simpler model), $-2\log(\Lambda)$ is asymptotically Chi-squared distributed with degrees of freedom equal to the difference in degrees of freedom between the models (Wilk's theorem). We can then compare the observed value of the statistic against what would be expected from this null distribution to compute a P value that represents how likely it would be to observe a result more extreme than the observed statistic under the null hypothesis. A permutation test was used to assess whether the maximally antagonistic alignment occurs at a lag that is different from zero for the temporal lag analysis (Fig. 5). This test computes the probability of the observed mean lag under the null distribution of mean lags that would be expected from a null hypothesis in which individual participant lags are randomly flipped in sign.

Reporting Summary. Further information on research design is available in the Nature Research Reporting Summary linked to this article.

Data availability

The data generated and analyzed in the current study are available from the corresponding author upon reasonable request.

Code availability

All analysis code is available from the corresponding author upon reasonable request.

References

51. Bollen, K. *Structural Equations with Latent Variables* (John Wiley, 1989).
52. Kline, R. B. *Principles and Practice of Structural Equation Modeling* (Guilford Publications, 2015).
53. Rosseel, Y. lavaan: an R package for structural equation modeling. *J. Stat. Softw.* **48**, 1–36 (2012).

Acknowledgements

The authors thanks A. Brennan and L. Alhussein for helpful discussions. This work was supported by the National Institutes of Health (NIH) grants R01 AG041878 and R01 NS105839 to M.A.S.

Author contributions

Y.R.M., S.W. and M.A.S. designed the experiments. Y.R.M. and M.A.S. analyzed the data and wrote the paper.

Competing interests

The authors declare no competing interests.

Additional information

Extended data is available for this paper at https://doi.org/10.1038/s41593-020-0600-3.

Supplementary information is available for this paper at https://doi.org/10.1038/s41593-020-0600-3.

Correspondence and requests for materials should be addressed to M.A.S.

Peer review information *Nature Neuroscience* thanks Joern Diedrichsen, Ned Jenkinson, and the other, anonymous, reviewer(s) for their contribution to the peer review of this work.

Reprints and permissions information is available at www.nature.com/reprints.

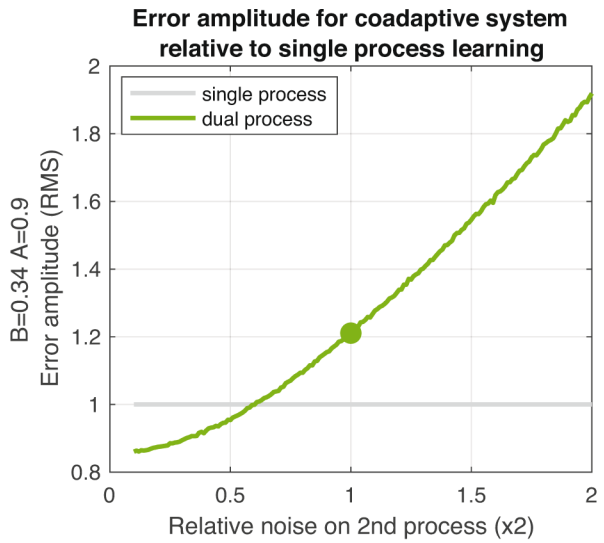

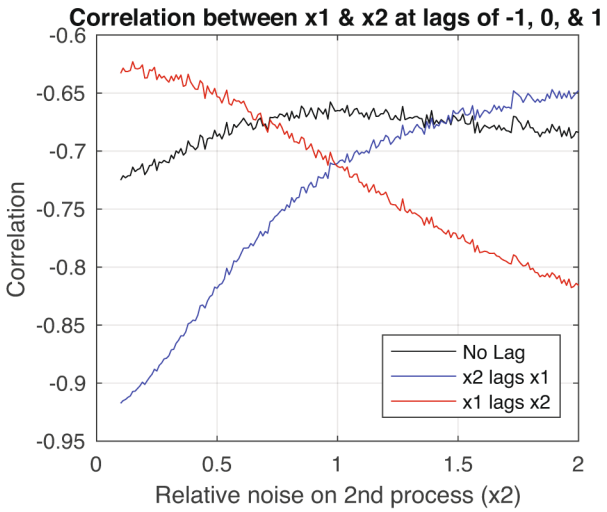

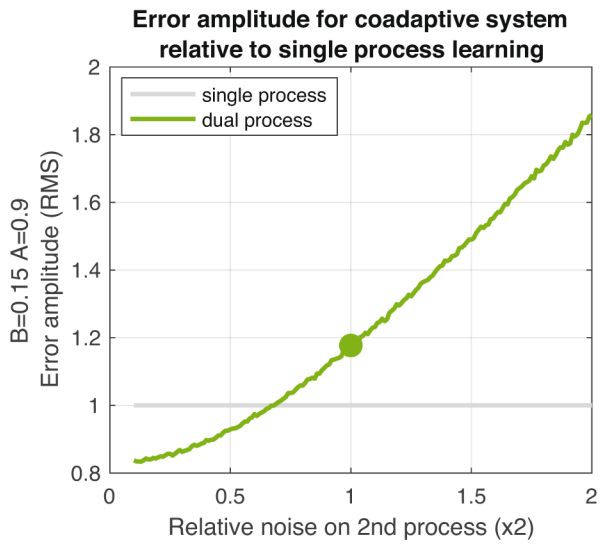

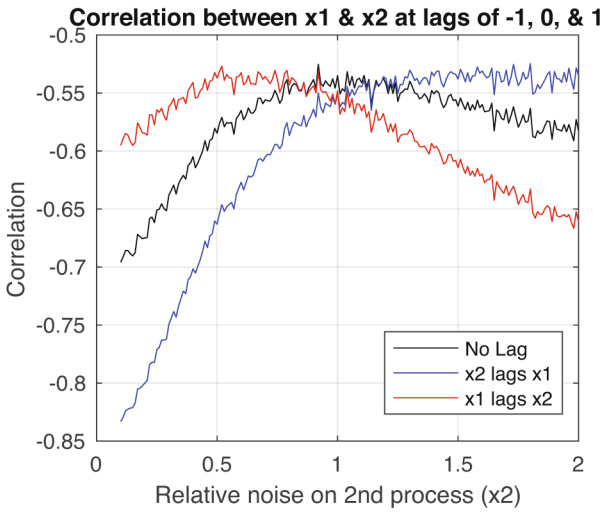

Extended Data Fig. 1 | The presence of time lag between adaptive responses is necessary to suppress the combined learning response at the perturbation-free frequencies in a two-process linear system. Left panel: Error amplitude resulting from the combination of both processes as a function of the relative noise level between processes. Right panel: Correlation between time series of processes when the processes are shifted from each other by −1, 0, or 1 trial. Black line indicates Lag-0 correlation. Blue line indicates Lag-1 correlation, that is corr(x2(n-1), x1(n)). Red line indicates Lead-1 correlation, that is corr(x2(n + 1), vs x1(n)). Thus the blue line being below the black & red indicates that x2 lags x1.

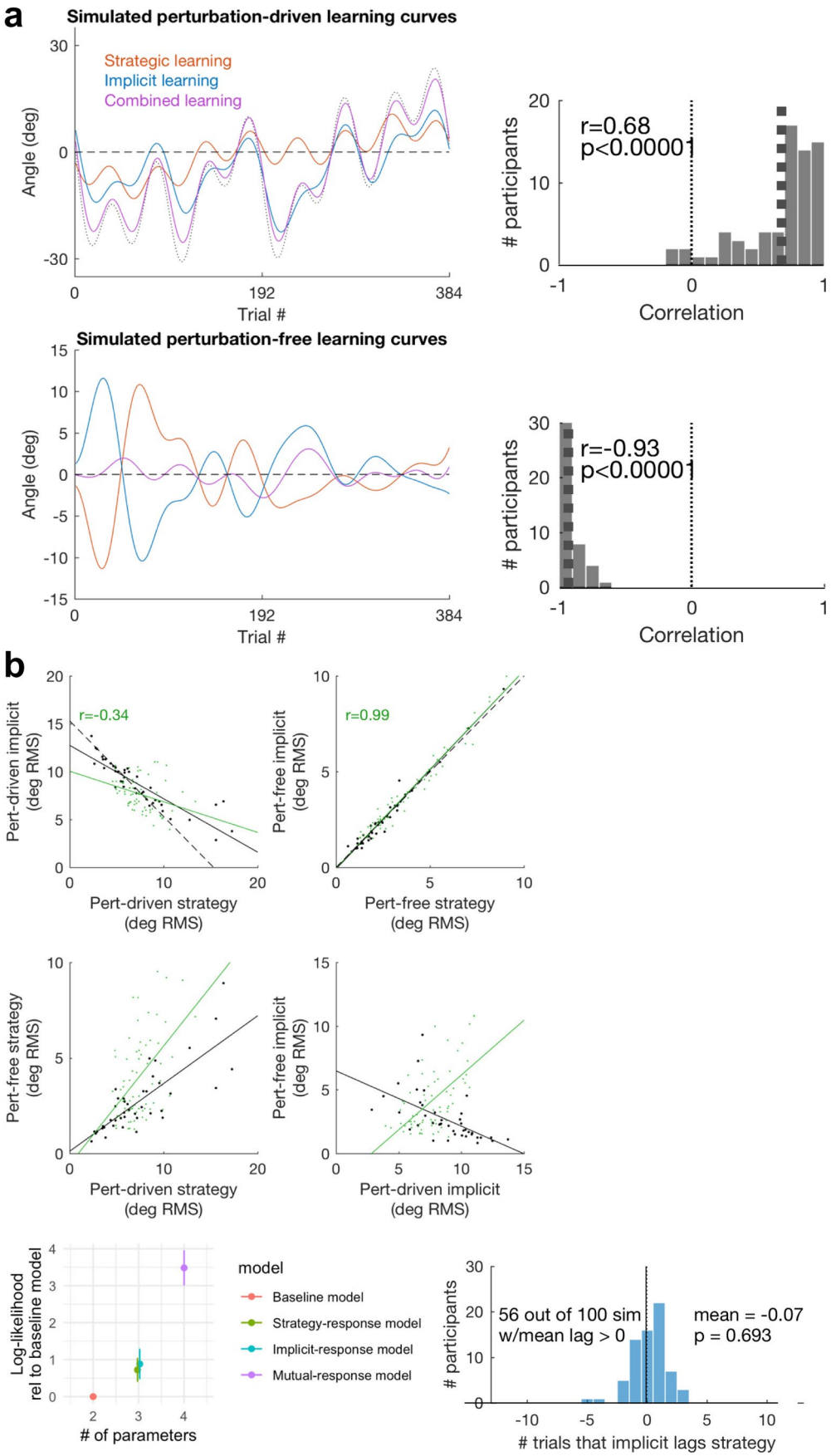

Extended Data Fig. 2 | See next page for caption.

Extended Data Fig. 2 | Simulation of two processes using *same* noise levels between processes and independently distributed learning rate parameters across participants. This simulation removes both the difference in noise levels and the across-participant learning rate anti-correlation from the simulation shown in Fig. 6 in the main paper. A_1=0.9, B_1=0.34+x_i, eps_1=1.75, A_2=0.9, B_2=0.34+y_i, eps_2=1.75, where x_i, y_i ~ Unif(−0.16, 0.16). Panels analogous to those in Fig. 6b, c in the manuscript. Upper left: simulated perturbation-driven learning curves for one example, simulated individual. Upper right: Histogram of simulated (n=69) within-participant correlations between perturbation-driven strategic and implicit learning curves. Lower left: analogous to upper left, but for perturbation-free learning curves. Lower right: analogous to upper right, but for perturbation-free learning curves. Please note that Supplementary Fig 1b on the following page presents panels analogous to those in Fig. 6d-f in the manuscript. Fig E1b. Simulation of two processes using same noise levels between processes and independently distributed learning rate parameters across participants (Like Supplementary Fig. 1a). This removes both the difference in noise levels and the across-participant learning rate anti-correlation from the simulation shown in Fig. 6 in the main paper. A_1=0.9, B_1=0.34+x_i, eps_1=1.75, A_2=0.9, B_2=0.34+y_i, eps_2=1.75, where x_i, y_i ~ Unif(−0.16, 0.16). Panels analogous to those in Fig. 6d–f in the manuscript. We performed 100 runs of the simulation, each with n=69. Top 2-by-2 panels: inter-individual relationships among perturbation-driven & perturbation-free strategic and implicit learning from one run of the simulation. Bottom left: log-likelihoods from the SEM analysis across 100 simulations (error bars indicate 95% CI, calculated across 100 simulations). Bottom right: histogram of lags from one run of the simulation. Text on histogram indicates the fraction of the 100 simulation runs for which the mean lag was greater than 0.

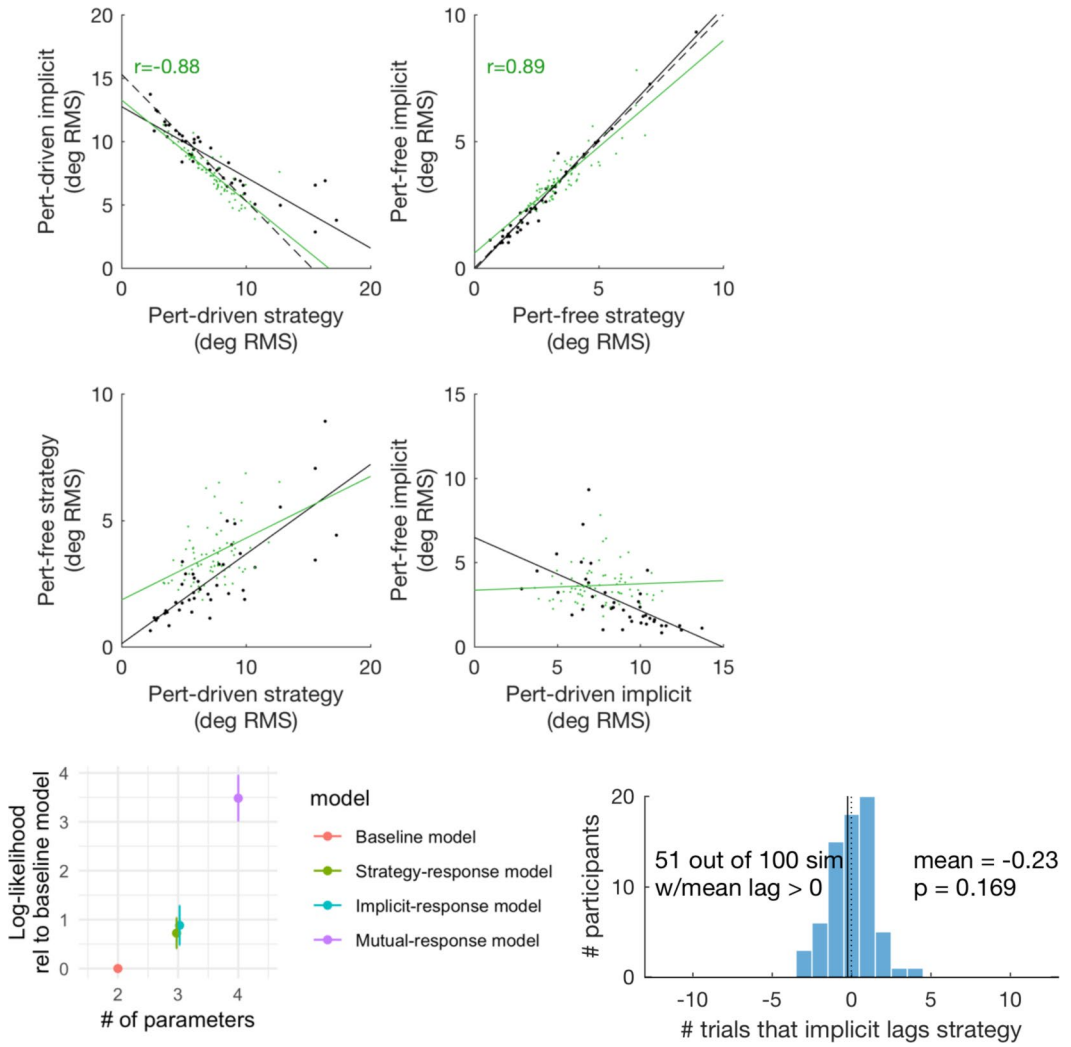

Extended Data Fig. 3 | Simulation of two processes using *same* noise levels between processes and anti-correlated learning rate parameters across participants. This simulation removes the difference in noise levels from the simulation shown in the main paper. A_1 = 0.9, B_1 = 0.34 + x_i, eps_1 = 1.75, A_2 = 0.9, B_2 = 0.34-x_i, eps_2 = 1.75, where x_i ~ Unif(−0.16, 0.16). Panels analogous to those of Supplementary Fig. 1b and Fig. 6d–f in the main paper.

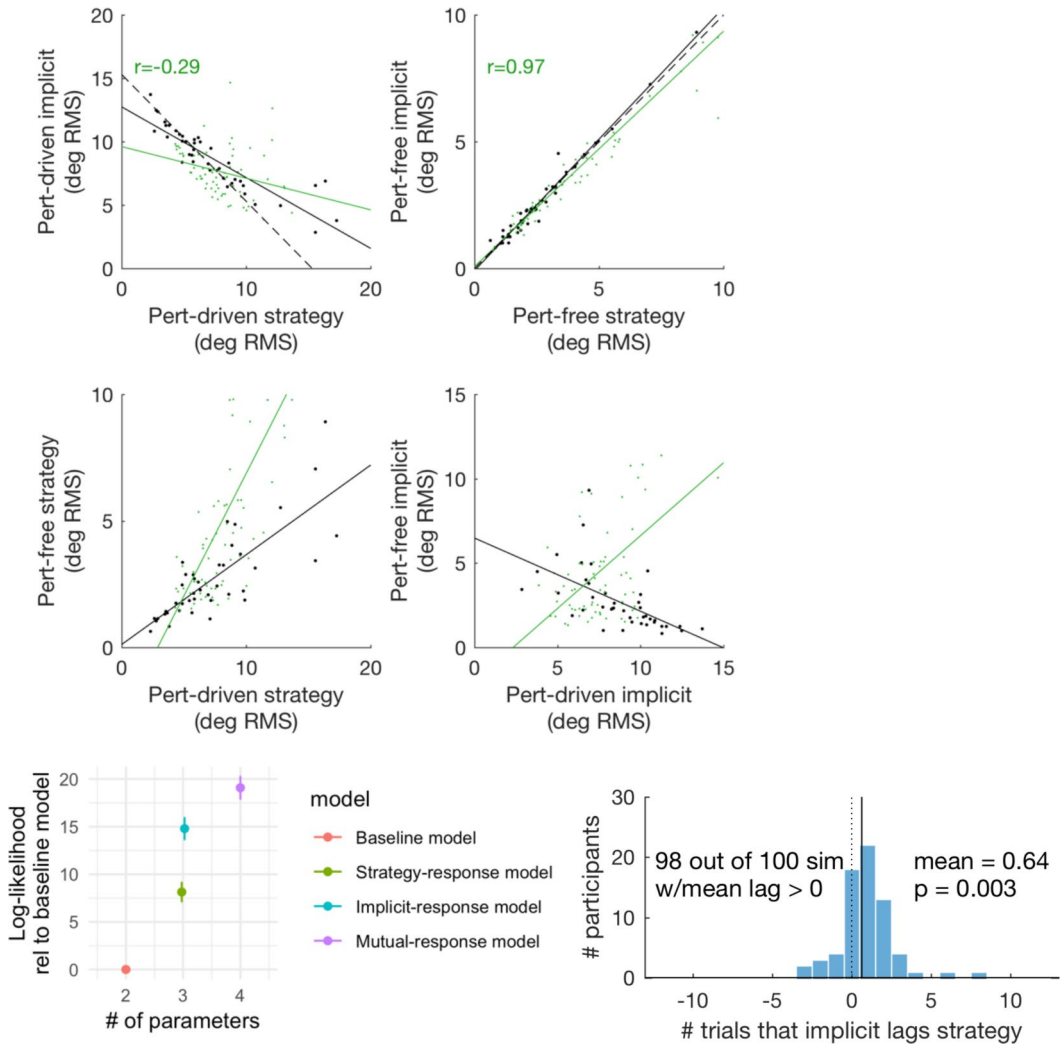

Extended Data Fig. 4 | Simulation of two processes using different noise levels between processes and independently distributed learning rate parameters across participants. This simulation removes the across-participant learning rate anti-correlation from the simulation shown in the main paper. A_1 = 0.9, B_1 = 0.34 + x_i, eps_1 = 1.5, A_2 = 0.9, B_2 = 0.34 + y_i, eps_2 = 2, where x_i, y_i ~ Unif(−0.16, 0.16). Panels analogous to those of Supplementary Fig. 2, 1b, and Fig. 6d–f in the main paper.

nature research

Corresponding author(s): Maurice Smith

Last updated by author(s): Jan 24, 2020

Reporting Summary

Nature Research wishes to improve the reproducibility of the work that we publish. This form provides structure for consistency and transparency in reporting. For further information on Nature Research policies, see Authors & Referees and the Editorial Policy Checklist.

Statistics

For all statistical analyses, confirm that the following items are present in the figure legend, table legend, main text, or Methods section.

n/a	Confirmed	
☐	☒	The exact sample size (*n*) for each experimental group/condition, given as a discrete number and unit of measurement
☐	☒	A statement on whether measurements were taken from distinct samples or whether the same sample was measured repeatedly
☐	☒	The statistical test(s) used AND whether they are one- or two-sided *Only common tests should be described solely by name; describe more complex techniques in the Methods section.*
☒	☐	A description of all covariates tested
☐	☒	A description of any assumptions or corrections, such as tests of normality and adjustment for multiple comparisons
☐	☒	A full description of the statistical parameters including central tendency (e.g. means) or other basic estimates (e.g. regression coefficient) AND variation (e.g. standard deviation) or associated estimates of uncertainty (e.g. confidence intervals)
☐	☒	For null hypothesis testing, the test statistic (e.g. *F*, *t*, *r*) with confidence intervals, effect sizes, degrees of freedom and *P* value noted *Give P values as exact values whenever suitable.*
☒	☐	For Bayesian analysis, information on the choice of priors and Markov chain Monte Carlo settings
☒	☐	For hierarchical and complex designs, identification of the appropriate level for tests and full reporting of outcomes
☒	☐	Estimates of effect sizes (e.g. Cohen's *d*, Pearson's *r*), indicating how they were calculated

Our web collection on statistics for biologists contains articles on many of the points above.

Software and code

Policy information about availability of computer code

Data collection	MATLAB R2010a, Psychophysics Toolbox for MATLAB v3.0, and custom matlab code
Data analysis	MATLAB R2015a and custom matlab code

For manuscripts utilizing custom algorithms or software that are central to the research but not yet described in published literature, software must be made available to editors/reviewers. We strongly encourage code deposition in a community repository (e.g. GitHub). See the Nature Research guidelines for submitting code & software for further information.

Data

Policy information about availability of data

All manuscripts must include a data availability statement. This statement should provide the following information, where applicable:

- Accession codes, unique identifiers, or web links for publicly available datasets
- A list of figures that have associated raw data
- A description of any restrictions on data availability

Provide your data availability statement here.

Field-specific reporting

Please select the one below that is the best fit for your research. If you are not sure, read the appropriate sections before making your selection.

☒ Life sciences ☐ Behavioural & social sciences ☐ Ecological, evolutionary & environmental sciences

For a reference copy of the document with all sections, see nature.com/documents/nr-reporting-summary-flat.pdf

Life sciences study design

All studies must disclose on these points even when the disclosure is negative.

Sample size	The sample sizes were determined based on pilot data and previous experience from similar experiments and are greater than those
Data exclusions	As described in the Methods, no participants were excluded from the dataset. Individuals trials with extreme values were excluded as outliers (19 out of 47616 trials, i.e. 0.04%), see Methods section.
Replication	The findings of Figs. 2-3 were replicated across 3 different experiments. Data was then pooled across these experiments for the subsequent analyses.
Randomization	Subjects were assigned to experiments based only on when they responded to advertisements about participation and their availability for scheduling, as in most cases, data were successively collected for different experiments. When different experiments were running concurrently, subjects were randomly assigned for participation.
Blinding	Investigators were aware of the experimental group assignments during the experiments and analysis. However, blinding was not applicable to this study, because none of the analysis were based on comparison of differences between participants in different experimental groups. Instead all analysis was within-participant and based on a frequency decomposition where information about each frequency depended on data from all trials from that participant.

Reporting for specific materials, systems and methods

We require information from authors about some types of materials, experimental systems and methods used in many studies. Here, indicate whether each material, system or method listed is relevant to your study. If you are not sure if a list item applies to your research, read the appropriate section before selecting a response.

Materials & experimental systems

n/a	Involved in the study
☒	☐ Antibodies
☒	☐ Eukaryotic cell lines
☒	☐ Palaeontology
☒	☐ Animals and other organisms
☐	☒ Human research participants
☒	☐ Clinical data

Methods

n/a	Involved in the study
☒	☐ ChIP-seq
☒	☐ Flow cytometry
☒	☐ MRI-based neuroimaging

Human research participants

Policy information about studies involving human research participants

Population characteristics	As described in the Methods, 69 individuals (49 female vs 20 male, mean age: 22.2 years) participated in the experiment. Participants had no known neurological conditions.
Recruitment	Participants were recruited from university advertisements.
Ethics oversight	Harvard University IRB

Note that full information on the approval of the study protocol must also be provided in the manuscript.